

SPHERE PACKINGS, V

SAMUEL L. P. FERGUSON

ABSTRACT. The Hales program to prove the Kepler conjecture on sphere packings consists of five steps, which if completed, will jointly comprise a proof of the conjecture. We carry out step five of the program, a proof that the local density of a certain combinatorial arrangement, the pentahedral prism, is less than that of the face-centered cubic lattice packing. We prove various relations on the local density using computer-based interval arithmetic methods. Together, these relations imply the local density bound.

1. INTRODUCTION

A collection of uniformly-sized balls in Euclidean 3-space is called a *packing* if no two balls have a common interior point. We refer to such a packing as a *sphere packing*. The Kepler conjecture asserts that the density of a packing of equal spheres in three-dimensions cannot exceed that of the face-centered cubic packing. Recently, Thomas C. Hales proposed a program designed to prove the Kepler conjecture [H1, H2, H3]. This program proposes a formulation designed to reduce the complexity of the problem to a level tractable via modern methods.

This formulation requires first that we define a decomposition of space, relative to a given packing of spheres. Next, we define stars, based on the decomposition. We then define a local density for these stars. Finally, we show that a sufficient local density bound for stars implies the required global density bound for the packing.

In addition to the formulation of the conjecture, the Hales program consists of five steps. An overview of the program detailing the content of each step can be found in [H3]. Details of the formulation itself can be found in [F&H]. We carry out step five of the program.

1.1. A Decomposition of Space. A decomposition of space, relative to a given packing of spheres, is critical to the formulation of the program. Our decomposition is inspired by the Delaunay and Voronoi decompositions, drawing from the advantages of each. We define a decomposition of space composed of a *Q-system* together with modified Voronoi cells called *V-cells*. We first define the *Q-system*, a partial decomposition of space, and then complete the decomposition by adding the *V-cells*.

Remark. There are many possible decompositions which could be used in a similar approach to the conjecture. The challenge is to select a decomposition which brings each element of the proof within reach. This selection has not been at all easy. For example, both the Delaunay and Voronoi decompositions have critical defects which prevent their use. The *Q-system* is so named because it consists of certain tetrahedrons called q.r. tets and quarters.

Date: May 8, 2019.

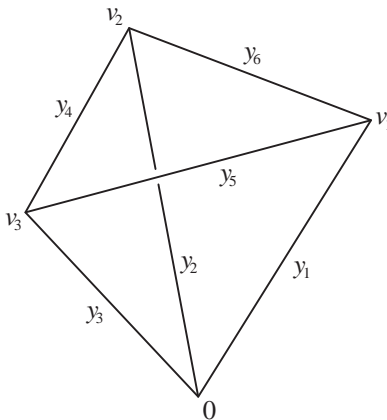


FIGURE 1. Tetrahedron with distinguished vertex and labeled edges.

We say that two sets *overlap* if their relative interiors intersect. To define the Q -system, we begin with an arbitrary saturated packing of spheres of radius one. We say that a packing is *saturated* if no more spheres may be added to the packing without overlapping spheres already in the packing. We consider only saturated packings, as we are looking for packings of maximal density. We identify the centers of the spheres as *vertices* of the packing. On occasion, we will distinguish a vertex of the packing, calling it the *origin*.

1.1.1. *Identification by edge lengths.* By connecting vertices in the packing, we can identify certain tetrahedrons. This identification is based on the length of the edges connecting the vertices. We label the edges and vertices of tetrahedrons as in Figure 1. Note that the order of the edge lengths determines which is the distinguished vertex of a tetrahedron.

1.1.2. *Quarters and q.r. tets.* We define two types of tetrahedrons, a *quasi-regular tetrahedron*, called a *q.r. tet*, and a *quarter*. A q.r. tet is a tetrahedron whose edge lengths each lie in the interval $[2, 2.51]$. A quarter is a tetrahedron with five edges with lengths in $[2, 2.51]$ and one long edge with length in $[2.51, 2\sqrt{2}]$.

If a vertex of a quarter is distinguished, the quarter has two orientations: flat, and upright. A quarter is said to be *flat* if the distinguished vertex is opposite the long edge. Similarly, a quarter is said to be *upright* if the distinguished vertex lies along the long edge. We refer to the long edge of a quarter as the *diagonal*.

Remark. Throughout this paper we introduce various special constants, such as 2.51. Although they may appear to be rather mundane numbers, these constants have been carefully selected. It is usually the case that our selection comes from a range of numbers. We tend to choose numbers which are easily represented in decimal form, although for some purposes, numbers with a simple binary representation would be better. We do not mean to imply that our computations are made to only two-digit significance, nor that the selection of constants is arbitrary.

1.1.3. *Octahedra.* If four quarters fit together along a common diagonal, forming a figure with six vertices, the resulting figure composed of quarters is called an *octahedron*. We use the term octahedron only when we refer to such a figure composed

of quarters. An octahedron may have more than one diagonal of length at most $2\sqrt{2}$, so the decomposition of an octahedron into quarters may not be unique.

1.1.4. *The Q -system.* The Q -system is a collection of non-overlapping q.r. tets and quarters. We construct the Q -system incrementally, building it from q.r. tets and quarters. To begin, we identify all q.r. tets, quarters, and octahedra in the packing. We will define the Q -system to be a subset of these structures. We consider each q.r. tet and quarter in turn, choosing which ones we will add to the Q -system.

We first consider all identified octahedra. For each octahedron in the packing, we fix a diagonal of length at most $2\sqrt{2}$, and place the four quarters along that diagonal in the Q -system. Next, we place all quasi-regular tetrahedra in the Q -system. By Lemmas 1.2 and 1.3 of [F&H], it is not possible for q.r. tets to overlap either themselves or octahedra.

Next, we wish to place the rest of the quarters into the Q -system. Unfortunately, there is some ambiguity about how to do this without overlapping the quarters.

Remark. The resolution of the ambiguities in placing quarters into the Q -system is tedious. Details can be found in [F&H].

We say that two tetrahedra are *adjacent* if they share a face.

The first ambiguity arises when we have two adjacent quarters, sharing a diagonal. If we identify their common vertex opposite the diagonal, they become flat quarters. It is possible that the same collection of vertices could be decomposed into two flat quarters with a different diagonal. We call this ambiguity a conflicting diagonal. It is not important for this paper which choice we make for the decomposition. Making a selection when necessary, we place the adjacent quarters which share a diagonal into the Q -system.

The second ambiguity which arises is the case of two isolated, overlapping quarters. By isolated we mean that neither is adjacent to another quarter with which it shares a diagonal. If such a case arises, we place neither quarter in the Q -system.

To complete the Q -system, we add all remaining unconsidered quarters, those which are isolated and which do not overlap anything else in the Q -system. This completes the definition of the Q -system.

1.1.5. *Voronoi cells.* The *Voronoi cell* at a vertex of the packing consists of all points in space which are closer to that vertex than any other vertex of the packing. The Voronoi decomposition of space is simply the collection of all Voronoi cells.

Remark. To define a V -cell at a vertex w , we could take the intersection of the Voronoi cell at w with the complement of the Q -system. However, this formulation leads to unnecessarily complex V -cells. This is due to the fact that a tetrahedron need not contain its circumcenter.

In order to define V -cells, we must first discuss the orientation of a vertex with respect to a face.

If the circumcenter of a tetrahedron S lies on the side of the plane P through the face of S opposite the vertex, we say that the face has *negative orientation* with respect to that vertex. To identify points lying on the side of P opposite the vertex, we say that these points lie on the *negative side* of the face. By Lemma 2.1 of [F&H], at most one face of a quarter or q.r. tet has negative orientation.

Remark. If a face of an element S of the Q -system has negative orientation, the Voronoi cell associated with the vertex of S opposite that face will pass through

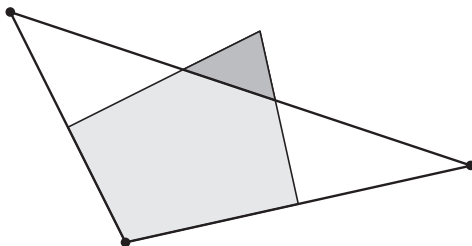


FIGURE 2. Two dimensional simplex with Voronoi cell.

the face, unless the Voronoi cell is truncated by a vertex outside of S . Hence the tip of the Voronoi cell protruding through the tetrahedron would be “orphaned” in the sense that the tip would be part of the star but not be contiguous with the rest of the Voronoi cell, since it will be separated by an element of the Q -system. By design, V -cells reappportion the protruding tip into the adjacent Voronoi cells so that we may avoid this complication.

1.1.6. *V-cells*. The construction of the V -cells is somewhat complex. We first describe a vertex deletion process, which we will use to construct the V -cells.

For each negatively-oriented tetrahedron S , we distinguish the vertex v opposite the negatively-oriented face.

We define the *tip* of the Voronoi cell associated with an isolated negatively-oriented tetrahedron S to be the part of the Voronoi cell determined by S alone which lies on the negative side of the face opposite v . Figure 2 represents the two-dimensional analog of a tip.

Each point x outside the Q -system lies in finitely many tips, each associated with a simplex S with distinguished vertex v . (Typically, this collection of vertices will be empty.) Temporarily deleting these vertices from the packing, we take the Voronoi decomposition of the remaining collection of vertices. The point x lies in the modified Voronoi cell at some new vertex u .

The deletion process therefore provides a mapping from the complement of the Q -system to the vertices of the packing.

We now consider a vertex w of the packing. We define the V -cell at w to be the set of points x outside the Q -system with the property that each lies in a modified Voronoi cell at w after the deletion process. That is, the V -cell at w is the pre-image of w under the mapping.

The collection of q.r. tets and quarters in the Q -system together with all the V -cells comprises our decomposition of space, relative to a fixed packing of spheres.

1.2. **Decomposition Stars.** Now that we have defined a decomposition of space relative to a packing, we can define a decomposition star relative to a vertex of the packing. We introduce the concept of a cluster of vertices, and then define a decomposition star in terms of the graph of the cluster.

We define the *height* of a vertex to be its distance from the origin.

Fix the origin at a vertex of the packing. Mark all vertices whose height is at most 2.51. The collection of marked vertices is called a *cluster*.

If the distance between two vertices in the cluster does not exceed 2.51, join them by an edge. We call the resulting structure the *graph* of the cluster.

Next, project the graph radially to the unit sphere centered at the origin. This projection produces a partition of the surface into regions called *standard regions*. By Lemma 3.10 of [H3], each edge projects to an arc on the unit sphere, and these arcs do not meet except at endpoints.

We say that a vertex is *enclosed* over a figure if the vertex lies in the infinite cone at the origin generated by the figure.

We associate a *decomposition star* with each vertex v . We define a decomposition star as the union of the V -cell at v with all the simplices in the Q -system having a vertex at v .

Decomposition stars and the standard regions have several important properties.

In the most general terms, we wish to show that V -cells, the Q -system and decomposition stars are compatible with standard regions. In the discussion which follows, we clarify this statement.

We will define two properties, each of which depends on the local nature of V -cells and the Q -system. These two properties define the compatibility of V -cells and the Q -system with standard regions.

The first property is that each q.r. tet or quarter of a decomposition star lies inside the cone over a single standard region.

The second property is somewhat harder to define.

We define a *quasi-regular face* to be a triangle constructed from vertices in the packing, whose edge lengths lie in the interval $[2, 2.51]$.

Note that a side of a standard region corresponds to a quasi-regular face.

By Lemma 2.2 of [F&H], if a vertex has negative orientation with respect to a quasi-regular face, it must form a q.r. tet with that face.

Using this information, we now consider the intersection of a V -cell with the cone over a standard region. We claim that the shape of the V -cell inside the cone is completely determined by the vertices lying inside the cone.

If a vertex w outside the cone is to affect the V -cell inside the cone, it must have negative orientation with respect to a quasi-regular face F corresponding to a side of the standard region. By the previous result, the vertex w must form a q.r. tet with a face of the standard region. See 2.2 of [H4].

By construction, if the Voronoi cell at w protrudes through F , the protruding part is attached to the V -cells inside the cone. Therefore the V -cell lying inside the cone over a standard region is completely determined by the vertices lying inside the cone.

Remark. These properties of standard regions allow us to consider each standard region in isolation. If this were not possible, the treatment of each decomposition star would be hopelessly complex.

1.2.1. *Standard clusters.* In our investigation of decomposition stars, we will need to consider the geometric arrangements associated with all possible standard regions. We call these arrangements standard clusters. We consider standard clusters in the context of decomposition stars.

Specifically, the *standard cluster* associated with a standard region R of a decomposition star is the union of the simplices in the decomposition star which lie in the cone over R together with the part of the V -cell that lies over R .

The standard cluster associated with a triangular standard region is a q.r. tet.

We call the standard cluster associated with a quadrilateral standard region a *quad cluster*.

1.2.2. *Classification of Quad Clusters.* Our treatment of decomposition stars requires that we classify all possible quad clusters.

Remark. We single out quad clusters because the decomposition star which we treat in this paper has only triangular and quadrilateral standard regions.

We call the four vertices of the packing which project to the vertices of the quadrilateral region the *corners* of the quad cluster.

We give two exhaustive lists of the possible decompositions, based on the length of the diagonals between the corners of a quad cluster.

If a quad cluster has a diagonal between two corners whose length does not exceed $2\sqrt{2}$, there are three possible decompositions.

First, the quad cluster could be composed of two flat quarters sharing the diagonal. We call this a *flat* quad cluster. Second, the quad cluster could be composed of two flat quarters sharing the other diagonal. Third, the quad cluster could be composed of four upright quarters forming an octahedron.

If both diagonals between the corners of a quad cluster have lengths which exceed $2\sqrt{2}$, there are again three possible decompositions.

First, the quad cluster could be an octahedron. Second, there could be no enclosed vertex of height at most $2\sqrt{2}$. We call such a quad cluster a *pure Voronoi* quad cluster, as it consists of only the part of the V -cell lying above the quadrilateral, since such a quad cluster cannot contain any quarters. Third, there could be an enclosed vertex of height at most $2\sqrt{2}$. We call such arrangements *mixed* quad clusters, since they consist of zero or more upright quarters and portions of V -cells lying above the quadrilateral.

1.3. **A Local Density Function.** The next element in our formulation is a local density function for decomposition stars.

We first construct a local density function for standard clusters. We will construct a local density function for decomposition stars by applying the local density function to each standard cluster in the star.

1.3.1. *The score of a standard cluster.* The *score* of a standard cluster represents one of many possible local density functions applied to a standard cluster. The choice of function depends on the geometry of the standard cluster in question. Our selection is made in an attempt to produce the best possible bounds on the local density.

In this paper we construct scoring functions only for q.r. tets and quad clusters. The scoring functions for other standard clusters can be found in other papers in the program.

We further subdivide our scoring functions, applying them to component quarters of quad clusters.

We define functions on tetrahedrons in terms of the edge lengths (y_1, \dots, y_6) of a tetrahedron. The first three edges y_1, y_2, y_3 are adjacent to the distinguished vertex or origin. Edge y_i lies opposite edge y_{i+3} for $i = 1, 2, 3$.

We use several distinct scoring functions. These functions are typically linear combinations of Voronoi volume and solid angle. To define these scoring functions, we require some intermediate definitions.

We define the solid angle $sol(S)$ of a tetrahedron S with distinguished vertex v to be three times the volume of the intersection of the unit ball at v with the infinite cone on S with origin at v . The units of solid angle are therefore steradians.

We define the geometric Voronoi volume of a tetrahedron S with distinguished vertex v to be the volume occupied by points of S lying closer to v than to the other vertices of the tetrahedron.

We define the analytic Voronoi volume $\text{vol}(S)$ of a tetrahedron S with distinguished vertex v to be the analytic continuation of the formula for the geometric Voronoi volume which holds when S contains its circumcenter. The analytic Voronoi volume is identical to the geometric Voronoi volume only when S contains its circumcenter. However, the sum of the analytic Voronoi volumes at all four vertices of S is equal to the volume of S .

Remark. This property allows us to produce a global density bound from a bound on the score of a decomposition star.

$$\text{Finally, let } \delta_{\text{oct}} = (\pi - 4 \arctan(\sqrt{2}/5))/(2\sqrt{2}).$$

1.3.2. *The score of a tetrahedron.* We define three scoring functions for tetrahedrons.

The simplest is called *vor* analytic or *vor*, taking its name from the analytic Voronoi volume. The *vor* analytic scoring $\text{vor}(S)$ of a tetrahedron S is given by $4(-\delta_{\text{oct}}\text{vol}(S) + \text{sol}(S)/3)$. Here *vol* denotes the analytic Voronoi volume at the distinguished vertex v .

Averaging $\text{vor}(S)$ over the two vertices adjacent to the long edge of an upright quarter gives *octavor*. That is, if the long edge of an upright quarter is y_1 ,

$$\text{octavor}(S) = (\text{vor}(y_1, y_2, y_3, y_4, y_5, y_6) + \text{vor}(y_1, y_5, y_6, y_4, y_2, y_3))/2.$$

The average of $\text{vor}(S)$ over all four vertices of a tetrahedron gives *gma*, which we also call the *compression* of a tetrahedron. That is,

$$\begin{aligned} \text{gma}(S) = & (\text{vor}(y_1, y_2, y_3, y_4, y_5, y_6) + \text{vor}(y_1, y_5, y_6, y_4, y_2, y_3) \\ & + \text{vor}(y_2, y_4, y_6, y_5, y_1, y_3) + \text{vor}(y_3, y_4, y_5, y_6, y_1, y_2))/4. \end{aligned}$$

Our method for choosing the scoring function for a particular tetrahedron depends on whether it is a q.r. tet or a quarter.

1.3.3. *Scoring a q.r. tet.* If the circumradius of a q.r. tet S is less than 1.41, we score S by compression. Otherwise, we score S using *vor* analytic.

1.3.4. *Scoring a quarter.* For quarters, the scoring system depends on both the orientation of the quarter and the circumradii of the faces adjacent to the diagonal. If the circumradius of each of the adjacent faces to the diagonal is less than $\sqrt{2}$, the quarter is scored using compression. Otherwise, flat quarters are scored using *vor* analytic, and upright quarters are scored using *octavor*.

1.3.5. *The score of V-cells.* The last element to be scored is the intersection of a V -cell with the cone over a standard region. Call this intersection S . Such elements are scored using Voronoi scoring. That is, they are scored using the usual formula $4(-\delta_{\text{oct}}\text{vol}(S) + \text{sol}(S)/3)$, where in this case $\text{vol}(S)$ represents the volume of S , and $\text{sol}(S)$ represents three times the volume of the intersection of S with the unit ball at the origin.

1.3.6. *Truncated Voronoi scoring.* If a quad cluster contains only vertices whose height exceeds $2\sqrt{2}$, we may bound the score of the quad cluster by using *truncated Voronoi*, meaning that the V -cell is truncated at a distance of $\sqrt{2}$ from the distinguished vertex. As this method decreases the volume term, it provides an upper bound on the Voronoi score. The bound on scoring is then $4(-\delta_{\text{oct}}\text{vol} + \text{sol}/3)$, where in this case, vol denotes the truncated Voronoi volume associated with the distinguished vertex, and sol denotes the solid angle associated with the distinguished vertex.

Remark. The selection of the scoring functions was a challenging part of the formulation of the problem. Compression arose as a natural local density function for the Delaunay decomposition. Similarly, vor arose as a local density function for the Voronoi decomposition. The scoring formulation which we exhibit is the result of much experimentation.

1.3.7. *Summary of functions.* We use the following functions: sol , the spherical angle associated with the distinguished vertex of a tetrahedron or quad cluster, dih , the dihedral angle associated with the first edge of a tetrahedron, vor , the vor analytic score of a tetrahedron, octavor , the averaged vor analytic score of an upright quarter, gma , the compression of a tetrahedron, and sc , a generic name for the score of a tetrahedron or quad cluster.

Explicit formulas for these special functions are available in [H3, H4, F&H].

Remark. We realize that our naming conventions are somewhat cumbersome. Initially, we gave traditional symbols to the special functions. For example, we referred to gma as Γ . However, as the library of functions increased, it became simpler to give each function a name which could be written easily in both *Mathematica* and C. Greek symbols do not have this property.

1.3.8. *The score of a decomposition star.* The score of a decomposition star is the sum of the scores of the standard clusters which comprise the star, such as q.r. tets and quad clusters.

1.3.9. *Definition of a point.* We find it useful to define a *point* to be the score of a regular tetrahedron (whose edge lengths are $(2, 2, 2, 2, 2, 2)$),

$$pt = 4 \arctan\left(\frac{\sqrt{2}}{5}\right) - \frac{\pi}{3}.$$

1.4. **The global density bound.** The final part of our formulation of the Kepler conjecture requires that we demonstrate how a scoring bound on all decomposition stars implies a global bound on the density of a packing.

Our formulation expresses the required global density bound of $\pi/\sqrt{18}$ in terms of a proposed bound on the score of a decomposition star. Together, the five steps in the Hales program will imply that the score of any decomposition star does not exceed 8 pt .

In order to produce the transition between local and global density bounds, we first discuss the essential equivalence of all of the scoring methods.

Recall that the analytic Voronoi decomposition of a tetrahedron produces a partition with four pieces. We compute the analytic Voronoi score of a tetrahedron using the analytic continuation of the volume of the piece containing the distinguished vertex. Adding these four (analytically continued) volumes gives the volume of the tetrahedron.

If we average sc over all vertices of a tetrahedron S , regardless of the scoring method, we arrive at $gma(S)$. In this sense, the different scoring schemes for tetrahedra are all equivalent. Recall that $gma(S)$ is a linear combination of the volume of S and the sum of the solid angles at each vertex of S . That is,

$$gma(S) = -\delta_{\text{oct}}\text{vol}(S) + \frac{1}{3} \sum_{i=1}^4 \text{sol}_i,$$

where sol_i represents the solid angle of S at vertex i .

Recall that the Voronoi score of a V -cell at a vertex w is

$$4(-\delta_{\text{oct}}\text{vol} + \frac{1}{3} \text{sol}),$$

where vol represents the volume of the V -cell and sol represents the solid angle at w of the V -cell.

Begin with a sphere of radius R , containing N vertices. Assume that the proposed bound,

$$sc \leq 8 \text{ pt},$$

holds for every decomposition star. Add this bound for every star in the sphere. Call the sum of the scores $\sum sc$. Each tetrahedron is shared by four stars. Therefore the contribution to $\sum sc$ from each tetrahedron S is $4 gma(S)$.

The volume terms add up to $\frac{4\pi}{3}R^3$ (neglecting the boundary), and the solid angles add to give $\frac{4\pi}{3}N$, the volume of the unit balls within the sphere of radius R . The boundary term is negligible as $R \rightarrow \infty$.

This gives, up to a negligible boundary term,

$$4(-\delta_{\text{oct}}\frac{4\pi}{3}R^3 + \frac{4\pi}{3}N) \leq 8N \text{ pt}.$$

The density of balls within the sphere (again, up to a negligible boundary term) is then

$$\frac{\frac{4\pi}{3}N}{\frac{4\pi}{3}R^3} \leq \frac{2\pi\delta_{\text{oct}}}{2\pi - 3 \text{ pt}}$$

Simplifying the right hand side, we find that it is equal to the desired bound, $\pi/\sqrt{18}$. Therefore the density of any packing cannot exceed the conjectured bound of $\pi/\sqrt{18}$.

For a more detailed account of this computation, see [H3, F&H].

Remark. The proposed 8 pt bound is achieved by the decomposition star of the face-centered cubic lattice packing. See Figure 3. This star is composed of 8 regular q.r. tets and 6 regular quad clusters. See Figure 4. Each q.r. tet in this star scores 1 pt , the maximum possible score of a q.r. tet. Each quad cluster scores 0 pt , the maximum score of a quad cluster. Hence the score of a face-centered cubic star is 8 pt .

2. THE PENTAHEDRAL PRISM

Having introduced our formulation of the Kepler conjecture, we can now define the subject of this paper, the pentahedral prism.

The pentahedral prism arises as a decomposition star in a saturated packing of 3-space with spheres of unit radius. It is a particular cluster with twelve vertices (not counting the origin). See Figure 5.

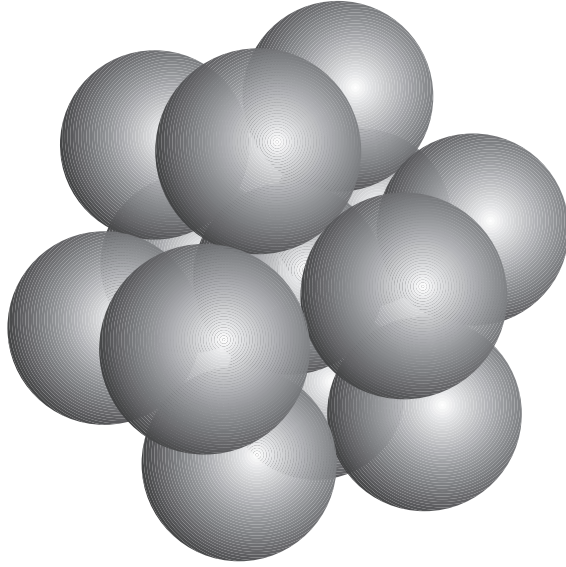


FIGURE 3. The face-centered cubic cluster.

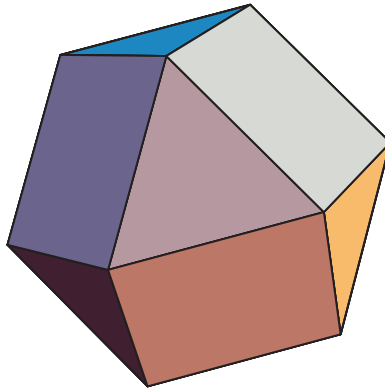


FIGURE 4. The face-centered cubic decomposition star.

The pentahedral prism is characterized by the arrangement and combinatorics of its standard regions. It is composed of ten triangular standard regions, and five quadrilateral standard regions. The ten triangles are arranged in two *pentahedral caps*, five triangles arranged around a common vertex. The five quadrilaterals lie in a band between the two caps. See Figure 6.

Recall that the standard cluster attached to a triangular standard region is a q.r. tet. Likewise, the standard cluster attached to a quadrilateral is a quad cluster. We use the term pentahedral cap to refer to both the standard regions and the q.r. tets which comprise it.

The five steps in the Hales program [H3] are

- I. A proof that even if all standard regions of a decomposition star are triangular the score is less than 8 *pt*.

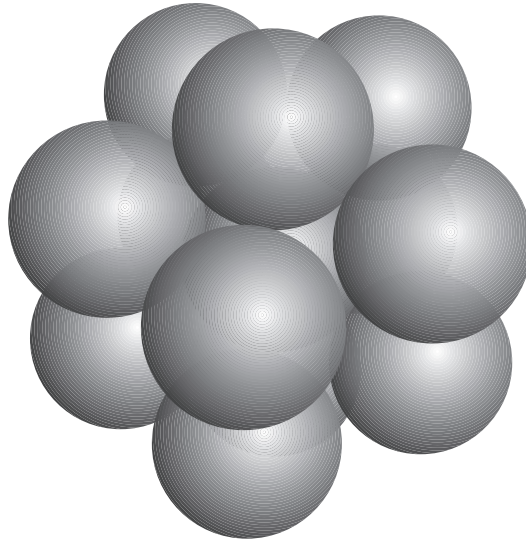


FIGURE 5. The pentahedral prism.

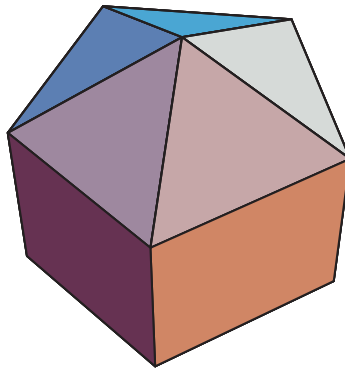


FIGURE 6. The faces of a pentahedral prism.

- II. A proof that standard clusters in regions of more than three sides score at most 0 pt .
- III. A proof that if all of the standard regions of a decomposition star are triangles or quadrilaterals, then the score does not exceed 8 pt (excluding the case of the pentahedral prism).
- IV. A proof that if some standard region has more than four sides, then the star scores less than 8 pt .
- V. A proof that the pentahedral prism scores less than 8 pt .

Remark. These steps were originally intended to be of roughly equal magnitude. Due to changes in our formulation of the decomposition of space and the local density function, some steps have become easier to complete than others.

In the earliest formulation, the pentahedral prism could score more than 8 pt . It appeared, on an experimental basis, to be the sole counterexample to the potential

success of the program. To a certain degree, the pursuit of a proof of step five drove the evolution of both the decomposition of space and the local density function.

The pentahedral prism still comes remarkably close to achieving the optimal local density, that achieved by the decomposition stars of the face-centered cubic lattice packing, which score 8 pt . In this sense, we consider the pentahedral prism to be a “worst case” decomposition star. As such, it required the devotion of much time and resources. Techniques which we developed to handle this case have proven to have significant impact on other steps of the program (as, conversely, techniques from other steps have affected this one).

Thus far, the relations required to treat the pentahedral prism have been delicate in contrast to the more general bounds which have to date sufficed to treat other decomposition stars.

As of this writing, steps I and II are complete [H3, H4]. Hales has exhibited partial results for III and IV.

Remark. The nomenclature for the star which we treat in step five is somewhat problematic. This object is a prism in only the weakest sense, technically speaking. In addition, it is denoted a “pentagonal prism” in [H3]. With a similar degree of inaccuracy, we could also call it a “pentangular prism”.

3. THE SCORING BOUND

We present computations using auxiliary bounds which imply the main result of the paper, that the score of the pentahedral prism is less than 8 pt .

We use the following lemma in proving almost all of the auxiliary bounds.

Lemma 3.1. *Pentahedral prisms which contain a q.r. tet whose score does not exceed -0.52 pt , or a quad cluster whose score does not exceed -1.04 pt , or a pentahedral cap whose score does not exceed 3.48 pt , must score less than 8 pt .*

Proof. We begin by recalling various bounds from other papers in the program. First, by Calculation 9.1 of [H3], $\text{gma}(S) \leq 1\text{ pt}$ for any q.r. tet S . Second, recall Lemma 9.17 of [H3], which states that if a q.r. tet has circumradius at least 1.41, meaning that it must be vor scored, then its score is less than -1.8 pt .

Together, these two results imply that the score of a q.r. tet cannot exceed 1 pt . Lemma 9.6 of [H3] states that if all of the q.r. tets in a pentahedral cap are scored by compression, the score of such a pentahedral cap is less than 4.52 pt . Therefore, we deduce that the score of any pentahedral cap is less than 4.52 pt .

By Lemma 3.13 of [F&H], the score of a quad cluster is nonpositive. Using the scoring bound for pentahedral caps together with this result, we conclude that a pentahedral prism must score less than 9.04 pt .

Therefore, if the score of a quad cluster does not exceed -1.04 pt , the score of the pentahedral prism to which it belongs must fall below 8 pt . Similarly, if the score of a q.r. tet does not exceed -0.52 pt , the score of the pentahedral cap containing it cannot exceed $(4 - 0.52)\text{ pt}$, bringing the score of the associated pentahedral prism below 8 pt , as the contribution from the other pentahedral cap is less than 4.52 pt . In particular, if any q.r. tet is vor scored, the score of the pentahedral prism to which it belongs must fall below 8 pt .

Likewise, if the score of a pentahedral cap does not exceed 3.48 pt , the score of the pentahedral prism with which it is associated must fall below 8 pt . \square

We restrict our attention to pentahedral prisms not treated by Lemma 3.1.

Remark. As usual, we have chosen the constant 4.52 *pt* as a relatively simple representative of many possible scoring bounds. We could prove a slightly tighter bound, but the resulting number would be more cumbersome.

We now present the main result of this paper.

Theorem 3.1. *The score of the pentahedral prism is less than 8 pt.*

Proof. We prove linear relations on all of the standard clusters in the pentahedral prism. We combine these relations to prove the required scoring bound. We invoke Lemma 3.1 repeatedly, in order to simplify the numerical verification of these relations.

In the section titled Computations, we establish

$$\text{sc} + m \text{sol} - b \leq 0,$$

for all quad clusters not treated by Lemma 3.1. Here *sc* denotes the score of a quad cluster, *sol* denotes the spherical angle associated with the quad cluster, $m = 0.3621$ and $b = 0.49246$.

In addition, we establish

$$\text{sc} + m \text{sol} + \epsilon \left(\text{dih} - \frac{2\pi}{5} \right) - b_c \leq 0$$

for all compression-scored q.r. tets forming part of a pentahedral cap not treated by Lemma 3.1. Here *dih* denotes the dihedral angle associated with the first edge of the tetrahedron (that is, the edge common to the five tetrahedra in a pentahedral cap), $\epsilon = 0.0739626$ and $b_c = 0.253095$.

Summing the relations for the five q.r. tets from a pentahedral cap, we find

$$\sum_{i=1}^5 \text{sc}_i + m \sum_{i=1}^5 \text{sol}_i + \epsilon \sum_{i=1}^5 \left(\text{dih}_i - \frac{2\pi}{5} \right) - 5b_c \leq 0.$$

Summing over both pentahedral caps and using the relation that the sum of the five dihedral angles in a pentahedral cap is 2π ,

$$\sum_{i=1}^5 \text{dih}_i = 2\pi,$$

we find

$$\sum_{i=1}^{10} \text{sc}_i + m \sum_{i=1}^{10} \text{sol}_i - 10b_c \leq 0.$$

We represent the tetrahedra from the second pentahedral cap by the indices $i = 6 \dots 10$.

Adding the relations for the five quad clusters (indexed from 11 to 15), and using the fact that the sum of the solid angles is 4π ,

$$\sum_{i=1}^{10} \text{sol}_i + \sum_{j=11}^{15} \text{sol}_j = 4\pi$$

we find

$$\sum_{i=1}^{10} \text{sc}_i + \sum_{j=11}^{15} \text{sc}_j + 4\pi m - 5b - 10b_c \leq 0.$$

Therefore,

$$sc \leq 5b + 10b_c - 4\pi m.$$

The left-hand side denotes the score of the pentahedral prism. If the right-hand side is bounded below $8 pt$, we have achieved the required result. Substituting the values of b, b_c, m , and pt , we find that the score of the pentahedral prism is less than $7.9997 pt$. \square

Remark. The majority of the bounds which we prove in this paper are “relaxed”, in the sense that they are ϵ -away from the ideal bound. By decreasing ϵ , we can prove tighter bounds, at the cost of increasing the complexity of the computer verifications.

We could prove a slightly tighter bound on quad clusters (by decreasing b). This would improve the bound on pentahedral prisms slightly, to $7.98 pt$, say.

4. INTERVAL ARITHMETIC

Due to the complex nature of the local density functions, it is typically unrealistic to attempt to prove the required relations directly. Instead, we prove the majority of the required relations via computer-based interval arithmetic methods.

We review the basic notions of interval arithmetic.

Suppose that the value of a function $f(x)$ lies in the interval $[a, b]$. Further, suppose that $g(x)$ lies in the interval $[c, d]$. Then $f(x) + g(x)$ must lie in $[a + c, b + d]$. While it may be the case that we could produce better bounds than this for the function $f + g$, these interval bounds give crude control over the behavior of the function. Interval arithmetic provides a mechanism for formalizing arithmetic on these bounds.

We represent an interval t as $[\underline{t}, \bar{t}]$. Then for intervals a and b ,

$$a + b = [\underline{a} + \underline{b}, \bar{a} + \bar{b}].$$

Likewise,

$$a - b = [\underline{a} - \bar{b}, \bar{a} - \underline{b}].$$

Multiplication is somewhat more complicated. Define

$$C = \{\underline{a}\underline{b}, \underline{a}\bar{b}, \bar{a}\underline{b}, \bar{a}\bar{b}\}.$$

Then

$$a * b = [\min(C), \max(C)].$$

We leave division as an exercise for the reader.

Similarly, we can define the operation of a monotonic function on an interval. For example,

$$\arctan(a) = [\arctan(\underline{a}), \arctan(\bar{a})].$$

Using interval arithmetic, we can produce crude bounds for polynomials evaluated on intervals. Likewise, we can produce crude bounds for rational functions evaluated on intervals. Finally, we add the composition of monotonic functions. This allows us to produce interval bounds for functions such as *sol* and *vor* over q.r. tets, quarters, or quad clusters.

5. THE METHOD OF SUBDIVISION

The relations on tetrahedra and quad clusters required for the scoring bound on decomposition stars typically have the form $g(y) \leq 0$ for $y \in I$, where I is a product of closed intervals. As g is usually continuous, the existence of a maximum is trivial. However, bounds on the behavior of g over all of I computed directly via interval arithmetic are generally poor.

We define a *cell* to be a product of closed intervals. By subdividing I into sufficiently small cells, the quality of the computed bounds on each cell usually improves enough to prove the relation for each cell, and hence for the original domain I .

If in fact $g(y) \leq c < 0$, this approach works very well. However, if the bound is tight at a point y_0 , i.e., $g(y_0) = 0$, then pure subdivision will usually fail, since the computed upper bound on g over any cell containing y_0 will typically be positive.

If y_0 is not an interior maximum, we turn to the partial derivatives of g . If we can show that the partials of g on a small cell containing y_0 have fixed sign (bounded away from zero), then the maximum value of g on that cell is easily computed. It is typically the case that a cell must be very small before we can determine the sign of the partials via interval arithmetic bounds.

6. DIMENSION REDUCTION

The relations on tetrahedra required for the scoring bound on decomposition stars are typically six-dimensional. For a quad cluster, they can be even higher-dimensional. For high-dimensional relations, the method of subdivision becomes very expensive, computationally speaking.

We define a simplification which reduces the dimension of the required computations. This simplification therefore reduces the computational expense of the verification of a relation.

We refer to this simplification as dimension-reduction. The details of the proof of the simplification vary depending on whether the scoring is by compression, vor analytic, or Voronoi.

Introduced in [H3] for compression scoring, this argument states that moving a vertex v_i along the edge $(0, v_i)$ toward the origin 0 holds the solid angle fixed, while increasing the score of the tetrahedron. See Figure 1. Since the reduction may be performed until an edge-length constraint is met, this argument reduces the number of free parameters for the verification, thus reducing the dimension and complexity of the verification of a relation.

The validity of the same reduction for vor analytic-scored tetrahedra is obvious if the tip of the Voronoi cell does not protrude. If the tip does protrude, we must use the analytic continuation for the Voronoi volume. In this case, the validity of the reduction is not obvious.

We provide a sketch of an analytic proof that this reduction increases the analytic Voronoi score of a tetrahedron. The geometric constraint of moving a vertex along an edge can easily be stated analytically in terms of the original edge lengths, $(y_1, y_2, y_3, y_4, y_5, y_6)$. This action depends on a single parameter, the distance of the vertex v_1 from the origin, which we call t . The new edge lengths are given by

$$(t, y_2, y_3, y_4, \sqrt{t^2 + y_3^2 - \frac{t(y_1^2 + y_3^2 - y_5^2)}{y_1}}, \sqrt{t^2 + y_2^2 - \frac{t(y_1^2 + y_2^2 - y_6^2)}{y_1}}).$$

Recall from [H3] that the formula for the analytic Voronoi volume is a rational function of χ , u , $\sqrt{\Delta}$, and x_i , where $x_i = y_i^2$. Further recall that χ , u , and Δ are all polynomial functions in x_i .

Substituting the computed edge lengths in the formula for the analytic Voronoi volume, taking the partial derivative with respect to t , replacing t with y_1 , multiplying by the positive term

$$8\sqrt{\Delta}u(x_1, x_3, x_5)u(x_1, x_2, x_6)/y_1,$$

and then simplifying, we end up with a large homogeneous polynomial in x_i of degree 6, which is too ugly to exhibit here (having 91 terms).

Evaluating this polynomial over all possible q.r. tets and quarters, we find that it is positive.

Therefore the volume is increasing in t , so to increase the score, we should push the vertex in along the edge. The verification of the sign of the polynomial is found in Calculation 9.6.1.

The validity of a similar reduction argument for Voronoi scoring of a quad cluster is obvious, since the Voronoi volume is increasing in t .

Remark. If the computational effort to prove the relations we require for the scoring bound on decomposition stars were not so extreme, we could dispense with the complications associated with dimension-reduction.

7. COMPUTATIONS

We derive the auxiliary bounds necessary to prove the scoring bound. We separate the bounds into sections, depending on the case to which each bound is to be applied.

Remark. We go to great lengths to reduce the complexity of the relations which we are required to verify. If we had sufficient computer resources, we could dispense with many of the methods which we use to reduce the complexity of the calculations. This would simplify the computations significantly. However, the majority of the relations which we wish to prove are complex enough that a direct approach rapidly overwhelms our available resources.

7.1. Quarters. We are required to prove that the score of a quarter is nonpositive.

Quarters are either flat or upright. Flat quarters are scored using either compression or vor analytic scoring. Upright quarters occurring in a quad cluster are scored using either compression or averaged vor analytic scoring. Recall the scoring scheme from 1.3.4 in the Introduction.

Since compression does not depend on a distinguished vertex, we need only consider the flat case. Calculation 9.1.1 shows that the compression score of any quarter is nonpositive.

Averaged vor analytic scoring, applied to an upright quarter, is similarly simple. Calculation 9.1.2 shows that the averaged vor analytic score of any upright quarter is nonpositive.

Remark. In these first two calculations, we have simplified the calculations by proving a stronger result than that which is strictly necessary. In the last case, we are required to fully invoke the scoring scheme. This complicates the analysis.

The only case remaining is that of a flat quarter, scored by vor analytic. This case is trickier, since it is not true that vor analytic is nonpositive on any flat quarter. Therefore, we must assume that one of the two faces adjacent to the diagonal has circumradius not less than $\sqrt{2}$. This constraint complicates the verifications.

We first consider a small cell containing the edge lengths $(2, 2, 2, 2, 2, 2\sqrt{2})$. We call a cell containing these edge lengths a *corner* cell. We prove in Calculation 9.1.3 that for a sufficiently small corner cell, the y_1 through y_5 partials (the edge lengths corresponding to the short edges) are negative.

To find the maximum score, we therefore decrease the short edges as much as possible, while not violating the face constraint. On such a cell, the face constraint of one of the edges is tight, so we may assume that $\eta(y_1, y_2, y_6) = \sqrt{2}$ and $y_3 = 2$, $y_4 = 2$, and $y_5 = 2$ or else $\eta(y_4, y_5, y_6) = \sqrt{2}$ and $y_1 = 2$, $y_2 = 2$, and $y_3 = 2$, where $\eta(y_1, y_2, y_3)$ is the circumradius of a face with edge lengths (y_1, y_2, y_3) .

We represent the desired relation as $sc + \alpha(\eta^2 - 2) \leq 0$ for $\alpha = 0.125$. Calculation 9.1.4 verifies this relation.

Second, we prove the desired relation off of the corner cell. We subdivide this verification into Calculation 9.1.5 taking advantage of dimension reduction and partial derivative information, and Calculation 9.1.6 which only considers the boundary (where the face constraint is tight).

7.2. Quasi-regular Tetrahedra. There are three verifications required to prove the desired relation on q.r. tets. First, we prove a relation between dihedral angle and score. We then show that if the dihedral angle of a tetrahedron in a pentahedral cap exceeds a certain bound, the score of the pentahedral cap must fall below $3.48\ pt$, falling into the purview of Lemma 3.1. We call such a bound a *dihedral cutoff*. This cutoff then allows us to prove the final bound.

In the following discussion, *dih* refers to the dihedral angle associated with the first edge of a q.r. tet, *sc* refers to the compression score of the tetrahedron, and *sol* refers to the solid angle at the distinguished vertex. We restrict our attention to q.r. tets whose score exceeds $-0.52\ pt$, as per Lemma 3.1.

The first relation has the form $sc \leq a_1\ dih - a_2$, where $a_1 = 0.3860658808124052$ and $a_2 = 0.4198577862$. Calculation 9.2.1 provides the verification of this relation.

Applying the relation to four q.r. tets forming part of a pentahedral prism, we find

$$\sum_{i=1}^4 sc_i \leq a_1 \sum_{i=1}^4 dih_i - 4a_2.$$

Applying the relation

$$dih_5 = 2\pi - \sum_{i=1}^4 dih_i$$

and adding sc_5 to both sides of the first relation, we find

$$\sum_{i=1}^5 sc_i \leq sc_5 + a_1(2\pi - dih_5) - 4a_2.$$

The left-hand side represents the score of the pentahedral cap. If the right-hand side does not exceed $3.48\ pt$, we can remove the arrangement from consideration, since it pulls the score of the associated pentahedral prism below $8\ pt$, as per Lemma 3.1.

We assert that if $\text{dih} \geq d_0$, where $d_0 = 1.4674$, the right-hand side

$$\text{sc}_5 + a_1(2\pi - \text{dih}_5) - 4a_2$$

does not exceed 3.48 pt . Rewriting this statement, we prove that $\text{dih} \geq d_0$ implies

$$\text{sc} - a_1 \text{ dih} \leq 3.48 \text{ pt} - 2\pi a_1 + 4a_2,$$

which is verified in Calculation 9.2.2. Hence we may restrict our attention to q.r. tets whose dihedral angle does not exceed the dihedral cutoff d_0 .

Using the dihedral cutoff, we establish the final relation,

$$\text{sc} + m \text{ sol} + \epsilon(\text{dih} - \frac{2\pi}{5}) - b_c \leq 0.$$

Calculation 9.2.3 provides the verification.

7.3. Flat Quad Clusters. Flat quad clusters are composed of two flat quarters, whose common face includes the long edge. We prove the relation $\text{sc} \leq -m \text{ sol} + b$ on quad clusters whose score exceeds -1.04 pt , again invoking Lemma 3.1. We arrive at this relation for flat quad clusters by proving the relation $\text{sc} \leq -m \text{ sol} + b/2$ on flat quarters. Here sc refers to vor or compression scoring, whichever is appropriate for the quarter.

We restrict our attention to flat quarters whose score exceeds -1.04 pt , recalling the fact that the score of flat quarters is non-positive. Adding the relation for each flat quarter, we arrive at the desired bound for flat quad clusters.

In the following discussion, we label the diagonal of a flat quarter y_6 .

Flat quarters may be scored using either compression or vor scoring. We treat each case separately.

First, suppose that we wish to prove the bound for compression scored quarters. This means that the circumradii of the two faces adjacent to the long diagonal do not exceed $\sqrt{2}$. We subdivide the verification into Calculation 9.3.1, a computation where we apply dimension-reduction and partial derivative information, and Calculation 9.3.2, a boundary verification, where we restrict our attention to cells which lie on the boundary between compression and vor scoring.

Second, we treat the vor-scoring case. In this case we prove the bound for vor-scored quarters. This means that at least one of the circumradii of the two faces adjacent to the long diagonal is at least $\sqrt{2}$. This verification is somewhat more complex than the compression case. We subdivide the verification into

1. Verification that the first three partials are negative on a small cell containing the corner (Calculation 9.3.3).
2. Verification of the bound on that small cell containing the corner, using the property that the first three partials are negative (Calculation 9.3.4).
3. A computation where we apply dimension-reduction and partial derivative reduction, omitting the corner cell (Calculation 9.3.5).
4. A boundary verification, where we restrict our attention to cells which lie on the boundary between compression and vor scoring, again omitting the corner cell (Calculation 9.3.6).

7.4. Octahedra. Recall that octahedra, a type of quad cluster, are composed of four upright quarters arrayed around their common long edge (known as the *diagonal*) so that each face containing the common edge is shared by two quarters.

We are required to prove a relation of the form

$$sc + m \text{ sol} - b \leq 0,$$

where sc denotes the score of an octahedron, sol denotes the solid angle associated with the distinguished vertex, and m and b are positive constants. By Lemma 3.1, we restrict our attention to octahedra whose score exceeds -1.04 pt .

Our treatment of octahedra, as usual, is comprised of a number of auxiliary computations. We prove bounds on upright quarters which are part of an octahedron, and then combine these bounds to deduce the required bound on octahedra in general.

Remark. Due to the complex nature of octahedra, we are required to consider a number of sub-cases, which we hope will not fatigue the reader. These cases are partitioned according to the length of the diagonal and the scoring system applied to the upright quarters.

Using a dihedral summation argument, we will eliminate octahedra whose diagonal lies in the range $[2.51, 2.716]$.

Next, we will treat the case where the diagonal lies in the range $[2.716, 2\sqrt{2}]$. Using a dihedral correction term, we will prove the bound for octahedra which are completely compression-scored, and octahedra which are completely vor-scored.

The remaining cases will consist of octahedra which contain either two or three vor-scored quarters. (Since a quarter is vor-scored if one of the faces containing the diagonal has circumradius $\sqrt{2}$ or greater, it is not possible for an octahedron to contain only one vor-scored quarter.) We treat these cases using an additional correction term.

The details follow.

In all computations involving octahedra, we label the diagonal y_1 .

In order to simplify the computations, we first prove an auxiliary cutoff bound. This first bound reduces the size of the cell over which we must conduct our search, as per Lemma 3.1.

Calculation 9.4.1 shows that if an upright quarter contains an edge numbered 2, 3, 5, or 6 whose length is not less than 2.2, its score is less than -0.52 pt .

Since such an edge is shared by another upright quarter in the same octahedron, the score of the associated octahedra must fall below -1.04 pt .

We restrict our search accordingly.

In the first case, we assume that the diagonal lies in the range $[2.51, 2.716]$. In Calculation 9.4.2, we prove a bound of the form

$$sc + c \text{ dih} \leq d$$

on upright quarters, where $c = 0.1533667634670977$, and $d = 0.2265$. Adding the bound for four quarters forming an octahedron, we find

$$\sum_{i=1}^4 sc_i + c \sum_{i=1}^4 \text{dih}_i \leq 4d.$$

Using the fact that the sum of the dihedral angles is 2π , we find that

$$sc \leq -2\pi c + 4d.$$

A computation involving the constants c and d shows that the score is less than -1.04 pt . Again invoking Lemma 3.1, we need only consider octahedra whose diagonal lies in the range $[2.716, 2\sqrt{2}]$.

Using this assumption, we prove bounds of the form

$$(1) \quad \text{sc} + m \text{ sol} + \alpha \text{ dih} \leq \frac{b}{4} + \alpha \frac{\pi}{2}$$

and

$$(2) \quad \text{sc} + m \text{ sol} + \alpha \text{ dih} + \beta x_1 \leq \frac{b}{4} + \alpha \frac{\pi}{2} + 8\beta,$$

where dih refers to the dihedral angle associated with the diagonal, sc refers to the scoring scheme appropriate for a particular upright quarter, and x_1 refers to the square of the length of the diagonal. We choose α and β according to the scoring scheme.

Remark. Appropriate values for the correction terms involving α and β were determined by experimentation.

Choosing $\alpha = 0.14$, we prove (1) for compression-scored quarters with diagonal in the interval $[2.716, 2\sqrt{2}]$ (Calculation 9.4.3). Using the same α , we prove (1) for vor-scored quarters with diagonal in the range $[2.716, 2.81]$ (Calculation 9.4.4).

Choosing $\alpha = 0.054$, $\beta = 0.00455$, we prove (2) for compression-scored quarters with diagonal in $[2.81, 2\sqrt{2}]$ (Calculation 9.4.5). Choosing the same α , but $\beta = -0.00455$, we prove (2) for vor-scored quarters with diagonal in $[2.81, 2\sqrt{2}]$ (Calculation 9.4.6).

Note that for vor-scored quarters, the first inequality is a relaxation of the second, since β is negative.

The verification of each of these inequalities involves a computation where we apply dimension-reduction and partial derivative information, and a boundary verification, where we restrict our attention to cells which lie on the boundary between compression and vor analytic scoring. Note that the dimension-reduction step for relation (2) is complicated by the presence of the βx_1 term.

Summing the first inequality over an octahedron, we find

$$\sum_{i=1}^4 \text{sc}_i + m \sum_{i=1}^4 \text{sol}_i + \alpha \sum_{i=1}^4 \text{dih}_i \leq b + 2\alpha\pi.$$

Using the fact that the dihedral angles sum to 2π , we find

$$\text{sc} + m \text{ sol} \leq b,$$

so octahedra with diagonals in the range $[2.716, 2.81]$ satisfy the requisite bound.

Summing the first inequality over a consistently scored octahedron (either all compression or all vor) with diagonal in the range $[2.81, 2\sqrt{2}]$, we again arrive at the desired bound.

The remaining cases involve octahedra which contain both compression and vor-scored quarters, and whose diagonals lie in the range $[2.81, 2\sqrt{2}]$. For this case, we use the second inequality.

The summation involving the second inequality is identical to the first, save for the presence of the β terms. If there are two vor-scored quarters and two compression-scored quarters, the beta terms cancel, giving the relation as before.

If there are three vor-scored quarters and one compression-scored quarter, we note that the same relation for vor-scored quarters holds if we replace β by $\beta/3$ (since we have now relaxed the bound). Summing the inequalities, the term involving β vanishes again, leaving the desired inequality.

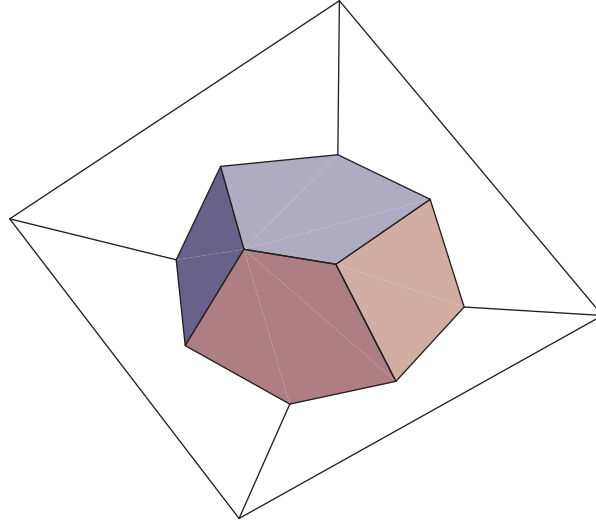


FIGURE 7. A pure Voronoi quad cluster.

7.5. Pure Voronoi quad clusters. The next class of quad clusters which we treat are the pure Voronoi quad clusters. We will define a truncation operation on these quad clusters. Truncation will simplify the geometry of the quad clusters, and will provide a convenient scoring bound. We will then divide our treatment of pure Voronoi quad clusters into two cases in order to simplify the analysis and numerical verifications as much as possible.

Recall from the classification of quad clusters (1.2.2) that a pure Voronoi quad cluster consists of the intersection of a V -cell at the origin with the cone at the origin over a quadrilateral standard region. We refer to the restriction of the V -cell to the cone over the quadrilateral as either the V -cell or the Voronoi cell of the quad cluster. Figure 7 describes the geometry of a simple V -cell.

In addition, recall that a vertex lying in the cone over a pure Voronoi quad cluster must have height greater than $2\sqrt{2}$. Such vertices can significantly complicate the geometry of the V -cell, affecting its shape and volume.

We remove the effect of vertices lying above a pure Voronoi quad cluster by removing all points from the V -cell which have height greater than $\sqrt{2}$. We call this operation *truncation at $\sqrt{2}$* . Truncation decreases the volume of the quad cluster. This decrease in volume increases the score of the quad cluster, bringing it closer to the proposed bound.

We refer to truncated pure Voronoi quad clusters as *truncated* quad clusters.

We define a scoring operation on pure Voronoi quad clusters which we call *truncated Voronoi* scoring. This operation consists of truncation at $\sqrt{2}$, followed by the usual Voronoi scoring.

Each diagonal across the face of a cluster must have length greater than $2\sqrt{2}$, otherwise we could form two flat quarters, contradicting the decomposition. We choose the shorter of the two possible diagonals, and will consider that diagonal in the analysis which follows.

We decompose the cluster into two tetrahedrons along the chosen diagonal. The face dividing the tetrahedrons is either acute or it is obtuse. We treat each case separately.

We must prove

$$sc + m \text{ sol} - b \leq 0,$$

where sc denotes the score of a pure Voronoi quad cluster, sol denotes the solid angle associated with the distinguished vertex, and m and b are positive constants. We call this relation a *bound* on the solid angle and score of a quad cluster. Invoking Lemma 3.1, we restrict our attention to quad clusters whose score exceeds -1.04 pt .

7.5.1. *The acute case.* If the separating face is acute, we prove

$$sc + m \text{ sol} - b/2 \leq 0$$

for each half independently, and deduce the desired bound by adding the bounds for each half. Since the score of each half is non-positive (by the arguments of Lemma 3.13 of [F&H]), we may restrict our attention to halves whose score exceeds -1.04 pt , by Lemma 3.1.

The required bound has the property that

$$m \text{ sol}_0 - b/2 \leq 0,$$

where sol_0 denotes the solid angle of the tetrahedron $(2, 2, 2, 2, 2, 2\sqrt{2})$. If $\text{sol} < \text{sol}_0$, then $m \text{ sol} < m \text{ sol}_0$, hence

$$m \text{ sol} - b/2 < m \text{ sol}_0 - b/2 \leq 0,$$

and

$$sc + m \text{ sol} - b/2 < sc \leq 0,$$

so the bound follows. We therefore may restrict our attention to halves whose solid angle is at least sol_0 . In addition, we restrict our attention to halves for which the dividing face is acute.

The required verifications for each half of an acute quad cluster are somewhat difficult to achieve directly, so we subdivide into a number of different cases in an attempt to reduce the complexity of the calculations. First, we show that the bound holds for all halves whose diagonal is at least 2.84 (Calculation 9.5.1). Using this information, we then prove the bound everywhere but in a small corner cell (Calculation 9.5.2). We then restrict our attention to the small corner cell (Calculation 9.5.3). These computations involve the use of partial derivative information, and include the required boundary computations.

7.5.2. *The obtuse case.* If the separating face is obtuse, the analysis becomes significantly harder. It is no longer possible to prove the desired bound on each half independently. The dimension of the full bound, even using the usual dimension-reduction techniques, is too high to make the verification tractable numerically. Therefore we adopt a different approach.

Using the dimension-reduction technique, we push each vertex along its edge until the distance from each vertex to the origin is 2. We call the resulting quad cluster a *squashed* cluster. Observe that the solid angle of the cluster is unchanged, while the volume of the Voronoi cell has decreased, thereby increasing the score of the cluster.

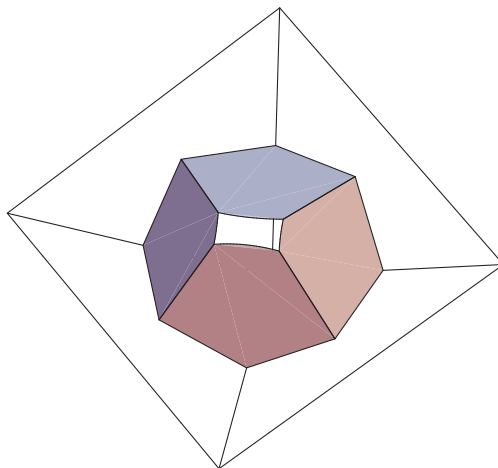


FIGURE 8. A typical truncated quad cluster.

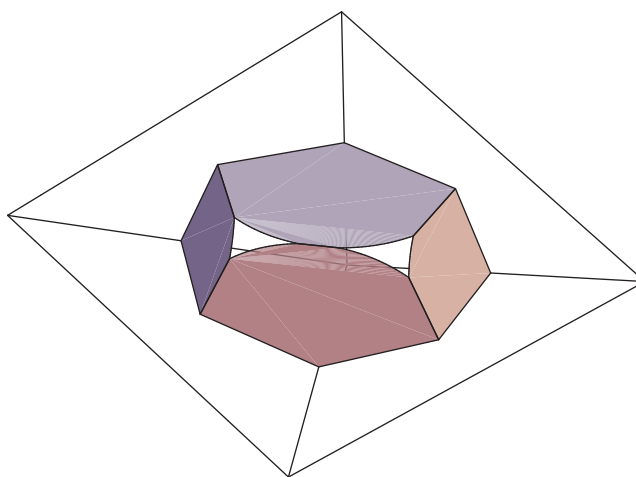


FIGURE 9. An impossible arrangement.

Since the central face is still obtuse, the length of the diagonal after this perturbation must still exceed $2\sqrt{2}$. Note, however, that the other edge lengths in the quad cluster can be as small as $4/2.51$.

The geometry of the V -cell of a squashed cluster, assuming that there is no truncation from vertices of the packing lying above the quad cluster, is that of Figure 7. When the V -cell is truncated at $\sqrt{2}$ from the origin, two potential arrangements arise. In the first arrangement, the truncated region is connected, as in Figure 8. In second potential arrangement, the truncated region is formed of two disjoint pieces, as in Figure 9.

We will conclude that the second, disjoint case cannot arise for squashed quad clusters. Suppose that it could. Pick an untruncated point along the central ridge of the V -cell (see Figure 9). The distance of this point from the origin is then less than $\sqrt{2}$, but due to its location on the central ridge, it is equidistant from the two

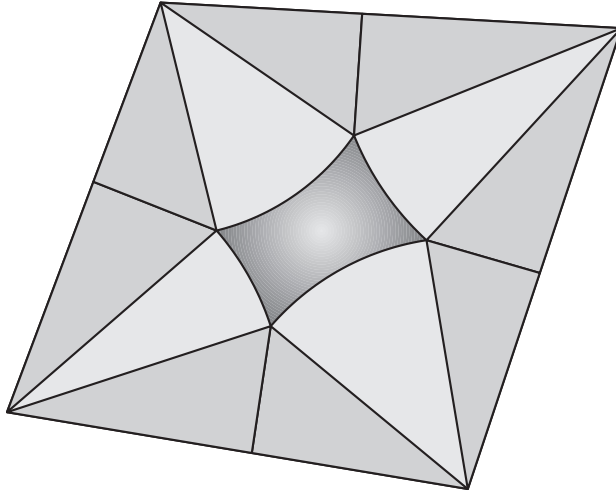


FIGURE 10. A representation of a truncated quad cluster.

nearest vertices and the origin. This implies that the circumradius of the resulting triangle must be less than $\sqrt{2}$, which contradicts the fact that the diagonals have length at least $2\sqrt{2}$.

7.5.3. *A geometric argument.* We introduce a simplification which will reduce the complexity of the obtuse case. This simplification will consist of a perturbation of the upper edge lengths of a squashed quad cluster. This perturbation will increase the score while holding the solid angle of the quad cluster fixed.

This simplification is based on a geometric decomposition of the truncated Voronoi cell. We will describe the decomposition, and then describe a construction which will ultimately simplify the analysis.

Remark. This simplification replaces the less-rigorous construction known as the “pizza” argument found in previous versions of this paper.

While our arguments will extend to treat a general squashed and truncated Voronoi cell associated with a general standard cluster, we restrict our attention to truncated Voronoi cells associated with quad clusters.

To begin, we consider the decomposition of a truncated Voronoi cell into its fundamental components. A truncated Voronoi cell is formed of three elements: a central spherical section (formed by the truncation), *wedges* of a right circular cone, and tetrahedrons called *Rogers simplices*.

We choose a representation of a truncated quad cluster composed of the radial projection of each element to a plane passing close to the four corners of the quad cluster. This decomposition is represented in Figure 10.

7.5.4. *Rogers simplices.* We now consider the geometry of the Rogers simplices.

Consider a face with edge lengths $(2, 2, t)$ associated with a side of a truncated quad cluster. Let b represent the circumradius of the face, and let r represent the orthogonal extension of a Rogers simplex from the face, as in Figure 11.

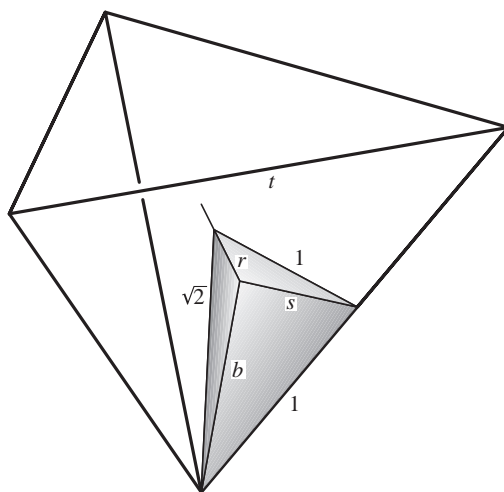


FIGURE 11. Detail of truncated Voronoi decomposition.

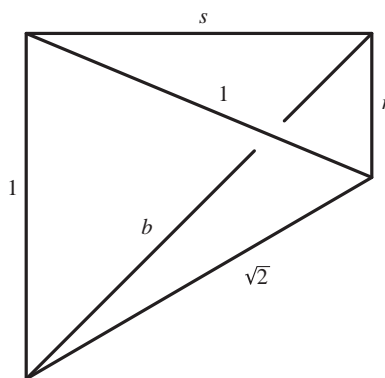


FIGURE 12. Detail of Rogers simplex.

Then

$$b = \frac{4}{\sqrt{16 - t^2}}$$

$$r = \sqrt{2 - b^2} = \sqrt{\frac{16 - 2t^2}{16 - t^2}},$$

and

$$s = \sqrt{b^2 - 1} = \frac{t}{\sqrt{16 - t^2}}.$$

See Figure 12.

7.5.5. *The geometric construction.* We now present the geometric construction which will imply the simplification.

We represent the geometry of the truncated Voronoi cell associated with one half of a quad cluster in Figure 13.

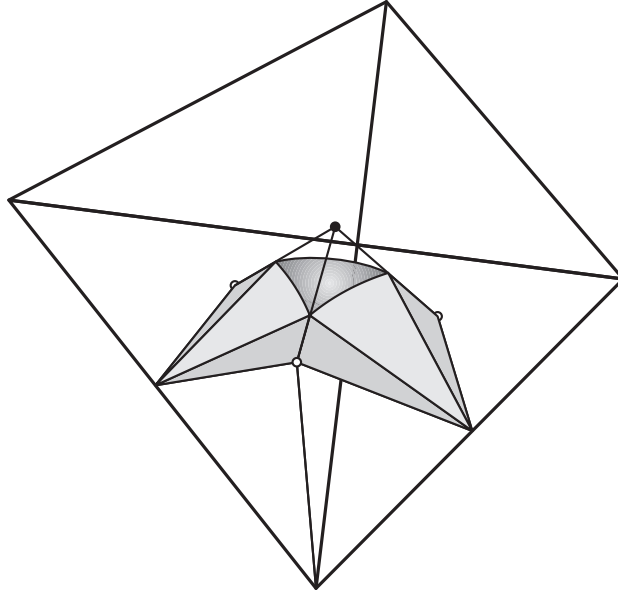


FIGURE 13. Decomposition of a truncated Voronoi cell.

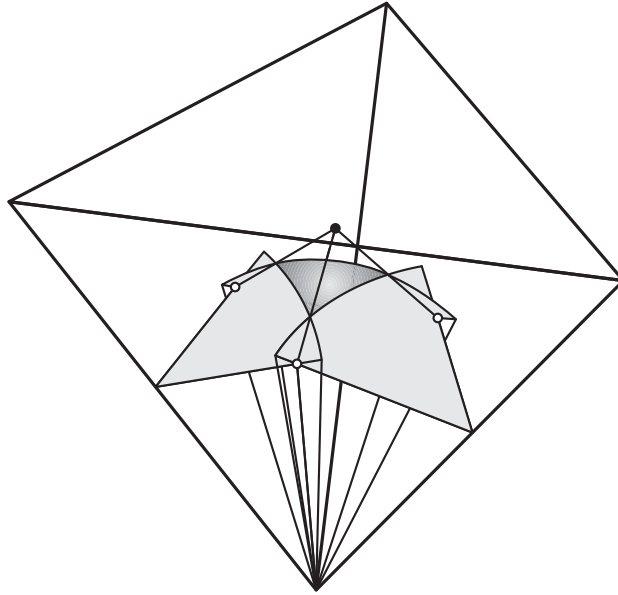


FIGURE 14. Wedges extended to include the Rogers simplices.

We can simplify the representation by extending the wedges to enclose the Rogers simplices. See Figure 14. This process adds an extra volume term.

The overlap between the wedges is slightly complicated. We simplify the overlap as follows. Take the cone over the overlap. Intersect it with a ball of radius $\sqrt{2}$ at the origin. We call the spherical sections produced by this construction *flutes*.

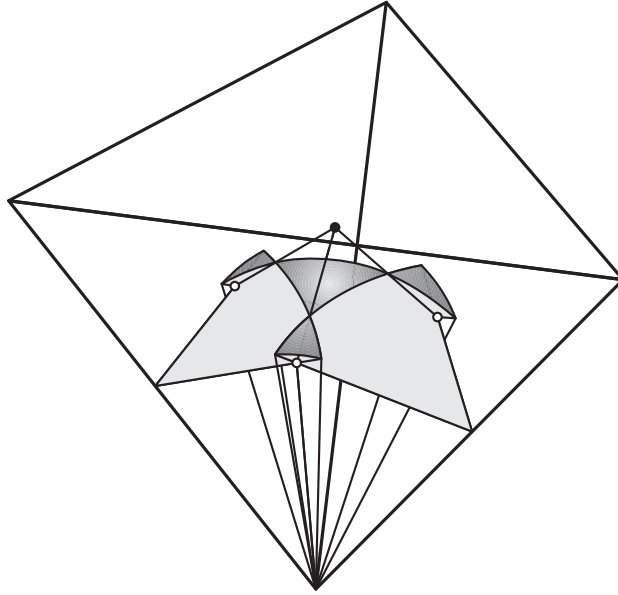


FIGURE 15. Decomposition with flutes.

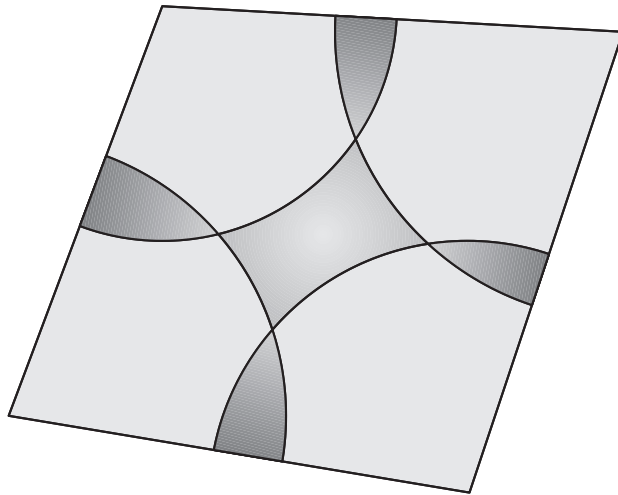


FIGURE 16. Planar representation with flutes.

This construction is represented in Figure 15. Figure 16 is a planar representation of this construction.

To form each flute, we have added two extra pieces of volume (per flute) to our construction. We call these pieces *quoins*. We attach each quoin to a Rogers simplex. See Figure 17.

7.5.6. *A solid angle invariant.* We now require some notation for the volumes which enter into this construction. Let c denote the volume of the central spherical angle.

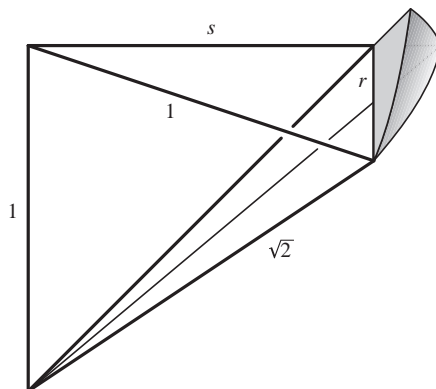


FIGURE 17. Detail of Rogers simplex with quoin.

Let r denote the volume of the Rogers simplices. Let w denote the volume of the wedges. Let w' denote the volume of the extended wedges. Let q denote the volume of the quoins. Let f denote the volume of the flutes. Finally, let v denote the volume of the truncated Voronoi cell. By the original decomposition,

$$v = c + r + w.$$

By our construction,

$$v = c + w' + q - f.$$

Recall that the solid angle s of the quad cluster is the sum of the dihedral angles minus 2π . The dihedral angles to which we refer are those associated with the edges between each corner of the quad cluster and the origin.

Our perturbation will hold the solid angle s of the quad cluster fixed. Therefore, the sum of the dihedral angles must also be fixed. This fixes w' .

Take the cone over each extended wedge and intersect it with a ball of radius $\sqrt{2}$ centered at the origin. Let t denote the sum of these volumes. Since the sum of the dihedral angles is fixed, t is also fixed.

Further, note that

$$\frac{2\sqrt{2}}{3}s = c + t - f.$$

This relation implies that $c - f$ is fixed. Combining this with the previous relations, we find that if we hold the solid angle fixed, the volume of the truncated Voronoi cell depends only on q , the volume of the quoins.

7.5.7. The quoin. We now develop a formula for the volume of a quoin. We first introduce some details of the Rogers simplices.

Consider a face $(2, 2, t)$ of a truncated quad cluster. Two Rogers simplices are associated with this face, as suggested in Figure 11. Observe that the volume of the quoin associated with one of these Rogers simplices is increasing in $r = \sqrt{\frac{16-2t^2}{16-t^2}}$. Next, observe that r is in turn decreasing in t . Therefore increasing t decreases the volume of the quad cluster, if we hold the solid angle fixed (by varying the length of another edge of the quad cluster).

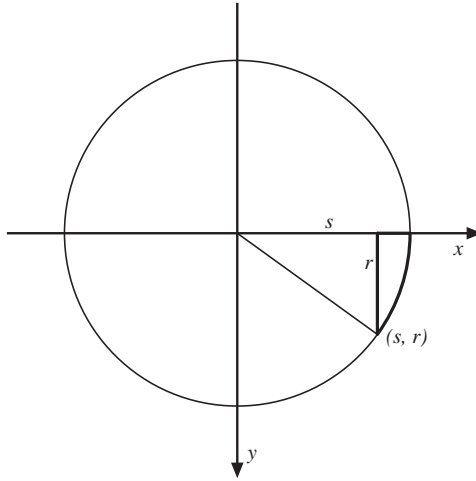


FIGURE 18. Top view of quoin.

Each half of a quad cluster has two variable edge lengths (not counting the shared diagonal). We label the variable edge lengths of one half of the quad cluster y_1 and y_2 . We label the length of the diagonal d . Holding the solid angle fixed, we may perturb one half by shrinking the larger and increasing the shorter length. We wish to establish that increasing the short length reduces the volume of the truncated Voronoi cell more than decreasing the longer length increases the volume.

7.5.8. *The volume of a quoin.* To achieve our reduction, we establish a formula for the volume of a quoin.

We then verify that the volume of the quoin associated with the shorter edge is decreasing faster under this perturbation than the volume of the quoin associated with the longer edge is increasing.

In other words, we wish to show that $y_1 < y_2$ implies that $V(y_1) + V(y_2(y_1))$ is decreasing in y_1 , or equivalently,

$$V_t(y_1) + V_t(y_2(y_1)) \frac{dy_2}{dy_1} < 0$$

where $V(t)$ is the volume of the quoin, $V_t(t)$ is the derivative of the volume, and y_2 is an implicit function of y_1 .

We construct the volume of a quoin by integrating the area of a slice. We place the quoin in a convenient coordinate system. See Figures 18 and 19. The truncating sphere has equation $x^2 + y^2 + z^2 = 2$. At the base of the quoin, $z = 1$, so $x = \sqrt{1 - y^2}$ gives the location of the right-boundary of the quoin. The plane forming the left face of the quoin is given by the equation $x = sz$, so the ridge of the quoin is given by the curve (su, y, u) , where $u = \sqrt{\frac{2 - y^2}{1 + s^2}}$.

Hence the area of a slice parallel to the x - z plane is given by the formula

$$A(t, y) = \frac{1}{2}(su - s)(u - 1) + \int_{su}^{\sqrt{1 - y^2}} (\sqrt{2 - x^2 - y^2} - 1) dx.$$

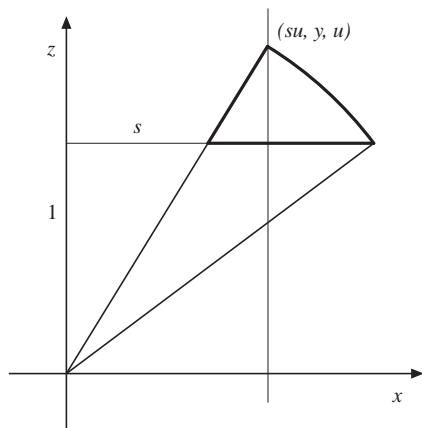


FIGURE 19. Side view of quoin.

The volume of a quoin is therefore given by the formula

$$V(t) = \int_0^r A(t, y) dy.$$

We actually only need to compute $V_t(t)$, which is fortunate, since the explicit formula for $V(t)$ is somewhat complicated. We have

$$V_t(t) = \int_0^r A_t(t, y) dy + A(t, r)r_t,$$

but $A(t, r) = 0$, so

$$V_t(t) = \int_0^r A_t(t, y) dy.$$

So in addition, we only need $A_t(t, y)$,

$$A_t(t, y) = \left(\frac{s}{2}(u^2 + 1) - \sqrt{1 - y^2} + \int_{\frac{1}{4}\sqrt{2-y^2}}^{\sqrt{1-y^2}} \sqrt{2 - x^2 - y^2} dx \right)_t,$$

so

$$A_t(t, y) = \left(\frac{s}{2}(u^2 + 1) \right)_t - \sqrt{2 - \frac{t^2}{16}(2 - y^2) - y^2} \frac{1}{4} \sqrt{2 - y^2}$$

which simplifies to

$$A_t(t, y) = \frac{8}{(16 - t^2)^{3/2}} - \frac{2 - y^2}{2\sqrt{16 - t^2}}.$$

Hence

$$V_t(t) = \frac{8r}{(16 - t^2)^{3/2}} - \frac{r}{\sqrt{16 - t^2}} + \frac{r^3}{6\sqrt{16 - t^2}},$$

which simplifies to

$$V_t(t) = \frac{-2\sqrt{2}(8 - t^2)^{3/2}}{3(16 - t^2)^2}.$$

7.5.9. *The solid angle constraint.* Holding the solid angle fixed, y_2 is an implicit function of y_1 . We now make that relation explicit. Using formulas from [H3], the solid angle constraint,

$$\text{sol}(2, 2, 2, y_1, y_2, d) = c,$$

where c is a constant, becomes

$$2 \arctan\left(\frac{\sqrt{\Delta}}{2a}\right) = c.$$

Let $x_1 = y_1^2$, $x_2 = y_2^2$, and $b = d^2$. Then

$$\Delta = -4b^2 - 4(x_1 - x_2)^2 + b(x_1(8 - x_2) + 8x_2),$$

and

$$a = 32 - d - x_1 - x_2.$$

So

$$\frac{-4b^2 - 4(x_1 - x_2)^2 + b(x_1(8 - x_2) + 8x_2)}{(32 - d - x_1 - x_2)^2} = c_1.$$

Therefore

$$\frac{dx_2}{dx_1} = -\frac{(16 - x_2)(x_2 + b - x_1)}{(16 - x_1)(x_1 + b - x_2)},$$

and

$$\frac{dy_2}{dy_1} = \frac{y_1}{y_2} \frac{dx_2}{dx_1},$$

hence

$$\frac{dy_2}{dy_1} = -\frac{y_1(16 - x_2)(x_2 + b - x_1)}{y_2(16 - x_1)(x_1 + b - x_2)}.$$

We return to the relation which we wish to prove, that $y_1 < y_2$ implies

$$V_t(y_1) + V_t(y_2) \frac{dy_2}{dy_1} < 0.$$

Note that all of the denominators are positive. Therefore clearing the denominators, we find that the desired relation is equivalent to

$$\begin{aligned} & -(8 - x_1)^{3/2}(16 - x_2)y_2(x_1 + b - x_2) + \\ & (8 - x_2)^{3/2}(16 - x_1)y_1(x_2 + b - x_1) < 0, \end{aligned}$$

or

$$\begin{aligned} & (16 - x_1)^2 x_1 (8 - x_2)^3 (b - x_1 + x_2)^2 < \\ & (16 - x_2)^2 x_2 (8 - x_1)^3 (b + x_1 - x_2)^2. \end{aligned}$$

If we define

$$g(x_1, x_2) = (16 - x_1)^2 x_1 (8 - x_2)^3 (b - x_1 + x_2)^2,$$

then the desired inequality is equivalent to $g(x_1, x_2) < g(x_2, x_1)$ for $x_1 < x_2$. There are several ways to prove this monotonicity relation. One is to prove that the polynomial

$$\frac{g(x_1, x_2) - g(x_2, x_1)}{8(x_1 - x_2)}$$

is positive for all allowable values for x_1 , x_2 , and b . Unfortunately, the resulting polynomial has degree 6, so the verification is somewhat unwieldy, although easy enough using interval methods.

A simpler method involves a factorization of g into g_1 and g_2 . We show that g_1 and g_2 each satisfy the monotonicity relation, and the relation then follows for g .

Define

$$g_1(x_1, x_2) = (16 - x_1)x_1(8 - x_2)(b - x_1 + x_2),$$

and

$$g_2(x_1, x_2) = (16 - x_1)(8 - x_2)^2(b - x_1 + x_2).$$

Clearly $g = g_1g_2$. We then construct the polynomials

$$p_1 = \frac{g_1(x_1, x_2) - g_1(x_2, x_1)}{x_1 - x_2}$$

and

$$p_2 = \frac{g_2(x_1, x_2) - g_2(x_2, x_1)}{x_1 - x_2}.$$

Simplifying p_1 and p_2 , we find that

$$\begin{aligned} p_1 = & 128b - 128x_1 - 8bx_1 + 8x_1^2 - 128x_2 \\ & + 32x_1x_2 + bx_1x_2 - x_1^2x_2 + 8x_2^2 - x_1x_2^2 \end{aligned}$$

and

$$\begin{aligned} p_2 = & -2048 + 192b + 320x_1 - 16bx_1 - 16x_1^2 + 320x_2 \\ & - 16bx_2 - 32x_1x_2 + bx_1x_2 + x_1^2x_2 - 16x_2^2 + x_1x_2^2. \end{aligned}$$

These polynomials are quadratic in x_1 and x_2 , and linear in b . The coefficient of b in p_1 is

$$128 - 8x_1 - 8x_2 + x_1x_2.$$

The coefficient of b in p_2 is

$$192 - 16x_1 - 16x_2 + x_1x_2.$$

Both coefficients are positive for x_1 and x_2 in $[16/2.51^2, 2.51^2]$. Therefore, the minimum values of p_1 and p_2 occur when b is at a minimum, $b = 8$.

The minimum value of each polynomial for values of x_1 and x_2 in the range $[16/2.51^2, 2.51^2]$ is now easily computed. Making the appropriate computations, we find that each polynomial is indeed positive. Hence the desired relation follows.

7.5.10. *The simplification.* We now apply the reduction argument. If we are not careful about how we apply the argument, however, this reduction could introduce some complications.

We begin with a squashed quad cluster with consecutive upper edge lengths (y_1, y_2, y_3, y_4) and diagonal d adjacent to the first two upper edges.

Recall that we chose the diagonal of the quad cluster to be the shorter of the two possible diagonals. We refer to the other possible diagonal as the *cross-diagonal*. Recall that the reduction fixes the length of the diagonal.

If the length of the cross-diagonal does not drop to $2\sqrt{2}$ under the perturbation, we arrive at the configuration with edge lengths (y'_1, y'_1, y'_2, y'_2) with diagonal d .

If the length of the cross-diagonal does drop to $2\sqrt{2}$, then stop the perturbation. This gives a quadrilateral (y'_1, y'_2, y'_3, y'_4) with diagonal $2\sqrt{2}$. Applying the perturbation to each half independently, we find that the score of each half is maximized by the configuration $(y''_1, y''_1, y''_2, y''_2)$ with diagonal $2\sqrt{2}$. We verify the relation for this arrangement in Calculation 9.5.5.

If the length of the cross-diagonal did not drop to $2\sqrt{2}$, switch to the cross-diagonal and repeat the process. If the (new) cross-diagonal does not drop to $2\sqrt{2}$, we have arrived at the configuration (y, y, y, y) with diagonal d' . Choose a new diagonal d'' to be the shorter of the two possible diagonals. We verify the desired relation for this arrangement in Calculation 9.5.4.

Finally, we make a few comments about extra constraints in the verifications.

Since the score of a quad cluster is non-positive, and $m(2 \text{sol}_0) - b \leq 0$ where $\text{sol}_0 = \text{sol}(2, 2, 2, 2, 2, 2\sqrt{2})$, we need only consider quad clusters for which the solid angle exceeds 2sol_0 .

The maximum length of the diagonal is $2.51\sqrt{2}$, since otherwise the triangles in the quadrilateral would be obtuse, forcing the cross-diagonal to be shorter than the diagonal. This would contradict our original choice of the shortest diagonal.

In Calculation 9.5.4, we assume that d is the shortest diagonal. Adding this constraint directly is tedious, since the formula for the cross-diagonal of the quad cluster is somewhat complicated. We apply a simpler but weaker constraint, that the diagonal d of a planar quadrilateral with edge lengths (y, y, y, y) is shorter than d' , the other planar diagonal. The constraint $d \leq d'$ gives the constraint $d^2 \leq 2y^2$. Since the cross-diagonal of the quad cluster is shorter than the cross-diagonal of the planar quadrilateral, this constraint is weaker.

7.6. Mixed Quad Clusters. By Proposition 4.1 of [F&H], the score of a mixed quad cluster is less than -1.04 pt . Therefore, we may discard all mixed quad clusters.

8. NUMERICAL CONSIDERATIONS

The verifications of the relations required in this paper appear intractable using traditional methods. Therefore, we use a relatively new proof technique, interval arithmetic via floating-point computer calculations.

Most real numbers are not representable in computer floating-point format. However, floating-point intervals may be found which contain any real number. Although the magnitude of real numbers representable in fixed-length floating-point format is finite, the format also provides for $\pm\infty$, which allows for interval containment of all reals. These intervals may be added, multiplied, etc., and the resulting intervals will contain the result of the operation applied to the real numbers which they represent.

Since floating-point arithmetic is not exact, interval arithmetic conducted using floating-point arithmetic is not optimal, in the sense that the interval resulting from an operation will usually be larger than the true resultant interval, due to roundoff. However, barring hardware or software errors (implementation errors, not roundoff errors), floating-point interval arithmetic, unlike floating-point arithmetic, is correct, in the sense that it provides correct interval bounds on the value of a computation, while floating-point arithmetic alone only provides an approximation to the correct value of a computation. We may therefore use interval arithmetic

to prove mathematical results. Floating-point arithmetic alone, in the absence of rigorous error analysis, cannot constitute a proof.

We implement floating-point interval arithmetic routines via the IEEE 754 Standard for floating-point arithmetic [IEEE].

Implementation of interval arithmetic is straightforward using directed rounding. In addition to arithmetic functions, we require interval implementations of the square root and arctangent functions. Fortunately, the IEEE standard provides the square root function. However, the arctangent function is somewhat problematic, since the standard math libraries do not provide explicit error bounds for their implementations of the arctangent function. In theory, they should provide an accuracy for the arctangent routine of 0.7 ulps, meaning that the error is less than one unit in the last place. I add interval padding of the form $[v - \epsilon, v + \epsilon]$, where v is the computed value, and $\epsilon = 2^{-49}$. This should be sufficient to guarantee proper interval containment, assuming that the library routines are correctly implemented.

Armed with standard interval arithmetic and interval arithmetic implementations of *sqrt* and *arctan*, we can implement interval arithmetic versions of all the special functions required for proving the sphere packing relations.

Evaluating these functions on cells, we get bounds. Unfortunately, these bounds are not very good. The bounds which we get from interval versions of the partial derivative functions are even worse. This means that cells have to be very small before we can draw conclusions about the signs of the partials. These bad bounds are due to the inherent nature of interval arithmetic—it produces worst-case results by design.

These bad bounds increase the complexity of the verifications tremendously. Some verifications, using these bounds, require the consideration of billions or trillions of cells, or worse. Therefore, we needed a method for producing better bounds than those which direct interval methods could provide.

The method which we eventually discovered is to use Taylor series. We compute explicit second (mixed) partial bounds for the major special functions, and use these bounds to produce very good interval bounds. These bounds are computed in Calculations 9.7.1 through 9.7.8. Essentially, the Taylor method postpones the error bound until the end of the computation, eliminating the error bound explosion which occurs with a straightforward interval method implementation.

9. CALCULATIONS

The following inequalities have been proved by computer using interval methods. Let $S = S(y) = S(y_1, \dots, y_6)$ denote a tetrahedron parametrized by the edge lengths (y_1, \dots, y_6) . In addition, we often parametrize by the squares of the edge lengths, (x_1, \dots, x_6) .

Recall from Section 3 that $m = 0.3621$, $b = 0.49246$, $\epsilon = 0.0739626$ and $b_c = 0.253095$.

9.1. Quarters.

Calculation 9.1.1. $\text{gma}(S) \leq 0$ for $y \in [2, 2.51]^5 [2.51, 2\sqrt{2}]$.

Calculation 9.1.2. $\text{octavor}(S) \leq 0$ for $y \in [2.51, 2\sqrt{2}] [2, 2.51]^5$.

Define the corner cell $C = [2, 2 + 0.51/16]^5 [2\sqrt{2} - (2\sqrt{2} - 2.51)/16, 2\sqrt{2}]$.

Calculation 9.1.3. $\frac{d}{dy_i} \text{vor}(S) < 0$ for $i = 1, \dots, 5$ and $y \in C$.

Calculation 9.1.4.

$$\text{vor}(S) + 0.125(\eta(y_1, y_2, y_6)^2 - 2) \leq 0$$

for $y_3 = y_4 = y_5 = 2$ and $y \in C$, and

$$\text{vor}(S) + 0.125(\eta(y_4, y_5, y_6)^2 - 2) \leq 0$$

for $y_1 = y_2 = y_3 = 2$ and $y \in C$.

Calculation 9.1.5. $\text{vor}(S) \leq 0$ for $y \in [2, 2.51]^5[2.51, 2\sqrt{2}]$, $y \notin C$, using dimension-reduction.

Calculation 9.1.6.

$$\text{vor}(S) \leq 0$$

for $y \in [2, 2.51]^5[2.51, 2\sqrt{2}]$, $y \notin C$ with

$$\eta(y_1, y_2, y_6)^2 = 2 \text{ or } \eta(y_4, y_5, y_6)^2 = 2,$$

not using dimension-reduction.

9.2. Quasi-regular Tetrahedra. Define $C = [2, 2.51]^6$, and recall

$$a_1 = 0.3860658808124052, a_2 = 0.4198577862, d_0 = 1.4674.$$

Calculation 9.2.1. Either

$$\text{gma}(S) \leq a_1 \text{dih}(S) - a_2$$

or

$$\text{gma}(S) \leq -0.52 \text{ pt}$$

for $y \in C$, using dimension-reduction.

Calculation 9.2.2. Either

$$\text{gma}(S) - a_1 \text{dih}(S) \leq 3.48 \text{ pt} - 2\pi a_1 + 4a_2$$

or

$$\text{dih}(S) < d_0$$

or

$$\text{gma}(S) \leq -0.52 \text{ pt}$$

for $y \in C$, using dimension-reduction.

Calculation 9.2.3. Either

$$\text{gma}(S) + m \text{sol}(S) + \epsilon(\text{dih}(S) - \frac{2\pi}{5}) - b_c \leq 0$$

or

$$\text{dih}(S) > d_0$$

or

$$\text{gma}(S) \leq -0.52 \text{ pt}$$

for $y \in C$, using dimension-reduction.

9.3. Flat Quad Clusters. Define $I = [2, 2.51]^5[2.51, 2\sqrt{2}]$, and define the corner cell

$$C = [2, 2 + 0.51/16]^5[2\sqrt{2} - (2\sqrt{2} - 2.51)/16, 2\sqrt{2}].$$

Calculation 9.3.1. Either

$$\text{gma}(S) + m \text{sol}(S) \leq b/2$$

or

$$\eta(y_1, y_2, y_6)^2 > 2$$

or

$$\eta(y_4, y_5, y_6)^2 > 2$$

or

$$\text{gma}(S) \leq -1.04 \text{ pt}$$

for $y \in I$, using dimension reduction.

Calculation 9.3.2. Either

$$\text{gma}(S) + m \text{sol}(S) \leq b/2$$

or

$$\eta(y_1, y_2, y_6)^2 = 2 \text{ with } \eta(y_4, y_5, y_6)^2 \leq 2,$$

or

$$\eta(y_4, y_5, y_6)^2 = 2 \text{ with } \eta(y_1, y_2, y_6)^2 \leq 2,$$

or

$$\text{gma}(S) \leq -1.04 \text{ pt}$$

for $y \in I$, not using dimension-reduction.

Calculation 9.3.3. $\frac{d}{dy_i} \text{vor}(S) < 0$ for $i = 1, 2, 3$ and $y \in C$.

Calculation 9.3.4. This computation is somewhat tricky, since the vor scoring constraint depends on both faces. The partial derivative information allows us to assume $y_3 = 2$. The rest of the analysis depends on which face is assumed to be large.

If the (y_1, y_2, y_6) face is large, the partial derivative information allows us to assume that the face constraint is tight, so $\eta(y_1, y_2, y_6)^2 = 2$. Therefore we can solve for y_1 in terms of y_2 and y_6 . We can apply partial derivative information for y_4 and y_5 . In this case, we prove

$$\text{vor}(S) + m \text{sol}(S) \leq b/2$$

for $y_3 = 2, y \in C$.

If the (y_4, y_5, y_6) face is large, we may assume that $y_1 = y_2 = 2$. We then prove

$$\text{vor}(S) + m \text{sol}(S) \leq b/2$$

or

$$\eta(y_4, y_5, y_6)^2 < 2$$

for $y_1 = y_2 = y_3 = 2, y \in C$.

Calculation 9.3.5. Either

$$\text{vor}(S) + m \text{sol}(S) \leq b/2,$$

or

$$\eta(y_1, y_2, y_6)^2 < 2 \text{ and } \eta(y_4, y_5, y_6)^2 < 2,$$

or

$$\text{vor}(S) \leq -1.04 pt$$

for $y \in I$, $y \notin C$, using dimension-reduction and partial derivative information.

Calculation 9.3.6. Either

$$\text{vor}(S) + m \text{sol}(S) \leq b/2,$$

with

$$\eta(y_1, y_2, y_6)^2 = 2 \text{ or } \eta(y_4, y_5, y_6)^2 = 2,$$

or

$$\text{vor}(S) \leq -1.04 pt$$

for $y \in I$, $y \notin C$, not using dimension-reduction.

9.4. Octahedra.

Calculation 9.4.1. We prove $\text{sc}(S) \leq -0.52 pt$, for each (appropriately scored) up-right quarter with edge lengths in the cell $[2.51, 2\sqrt{2}][2.2, 2.51][2, 2.51]^4$.

Calculation 9.4.2. Recall $c = 0.1533667634670977$, and $d = 0.2265$. We prove

$$\text{gma}(S) + c \text{dih}(S) \leq d$$

or

$$\text{gma}(S) \leq -1.04 pt$$

for $y \in [2.51, 2.716][2, 2.2]^5$. Note that for both faces adjacent to the diagonal,

$$\max \eta^2 = \eta(2.2, 2.2, 2.716)^2 < 2,$$

so all quarters in this cell are compression-scored. We make use of dimension-reduction.

Calculation 9.4.3. We prove

$$\text{gma}(S) + m \text{sol}(S) + \alpha \text{dih}(S) \leq \frac{b}{4} + \alpha \frac{\pi}{2}$$

or

$$\text{gma}(S) \leq -1.04 pt$$

for all compression-scored quarters $S(y)$, where $\alpha = 0.14$,

$$y \in [2.716, 2\sqrt{2}][2, 2.2]^2[2, 2.51][2, 2.2]^2.$$

We use dimension-reduction.

Calculation 9.4.4. We prove

$$\text{vor}(S) + m \text{sol}(S) + \alpha \text{dih}(S) \leq \frac{b}{4} + \alpha \frac{\pi}{2}$$

or

$$\text{vor}(S) \leq -1.04 \, pt$$

for all vor analytic-scored quarters $S(y)$, where $\alpha = 0.14$,

$$y \in [2.716, 2.81][2, 2.2]^2[2, 2.51][2, 2.2]^2.$$

Calculation 9.4.5. We prove

$$\text{gma}(S) + m \text{sol}(S) + \alpha \text{dih}(S) + \beta x_1 \leq \frac{b}{4} + \alpha \frac{\pi}{2} + 8\beta$$

or

$$\text{gma}(S) \leq -1.04 \, pt$$

for all compression-scored quarters $S(y)$, where $\alpha = 0.054$, $\beta = 0.00455$, $x_1 = y_1^2$, and

$$y \in [2.81, 2\sqrt{2}][2, 2.2]^2[2, 2.51][2, 2.2]^2.$$

We use some dimension-reduction.

Calculation 9.4.6. We prove

$$\text{vor}(S) + m \text{sol}(S) + \alpha \text{dih}(S) + \beta x_1 \leq \frac{b}{4} + \alpha \frac{\pi}{2} + 8\beta$$

or

$$\text{vor}(S) \leq -1.04 \, pt$$

for all vor analytic-scored quarters $S(y)$, where $\alpha = 0.054$, $\beta = -0.00455$, $x_1 = y_1^2$, and

$$y \in [2.81, 2\sqrt{2}][2, 2.2]^2[2, 2.51][2, 2.2]^2.$$

9.5. Pure Voronoi Quad Clusters. Recall sol_0 denotes the solid angle of the tetrahedron $(2, 2, 2, 2, 2, 2\sqrt{2})$.

Define the corner cell $C = [2, 2 + 0.51/8]^5[2\sqrt{2}, 2.84]$. We denote truncated Voronoi scoring by sc . The constraint that the dividing face be acute translates into $x_1 + x_2 - x_6 \geq 0$. In each computation we apply dimension-reduction.

We begin with the acute case.

Calculation 9.5.1. We prove

$$\text{sc}(S) + m \text{sol}(S) - b/2 \leq 0$$

or

$$\text{sol}(S) < \text{sol}_0$$

or

$$x_1 + x_2 - x_6 < 0$$

or

$$\text{sc}(S) \leq -1.04 \, pt$$

for $y \in [2, 2.51]^5 [2.84, 4]$.

Calculation 9.5.2. We prove

$$\text{sc}(S) + m \, \text{sol}(S) - b/2 \leq 0$$

or

$$\text{sol}(S) < \text{sol}_0$$

or

$$x_1 + x_2 - x_6 < 0$$

or

$$\text{sc}(S) \leq -1.04 \, pt$$

for $y \in [2, 2.51]^5 [2\sqrt{2}, 2.84]$ with $y \notin C$.

Calculation 9.5.3. We prove

$$\text{sc}(S) + m \, \text{sol}(S) - b/2 \leq 0$$

or

$$\text{sol}(S) < \text{sol}_0$$

or

$$x_1 + x_2 - x_6 < 0,$$

$y \in C$.

Finally, we consider the obtuse case.

Calculation 9.5.4. We prove

$$\text{sc}(S) + m \, \text{sol}(S) - b/2 \leq 0$$

or

$$\text{sol}(S) < \text{sol}_0$$

or

$$\text{sc}(S) \leq -0.52 \, pt$$

or

$$2y^2 < d^2$$

for a symmetric pure Voronoi quad cluster composed of two copies of S , where

$$S = (2, 2, 2, y, y, d),$$

$y \in [4/2.51, 2.51]$ and $d \in [2\sqrt{2}, 2.51\sqrt{2}]$.

Calculation 9.5.5. We prove

$$\text{sc}(S_1) + \text{sc}(S_2) + m(\text{sol}(S_1) + \text{sol}(S_2)) - b \leq 0$$

or

$$\text{sc}(S_1) + \text{sc}(S_2) \leq -1.04 \text{ pt}$$

or

$$\text{sol}(S_1) + \text{sol}(S_2) < 2 \text{sol}_0$$

for a pure Voronoi quad cluster composed of two tetrahedrons S_1 and S_2 , where

$$S_i = (2, 2, 2, y_i, y_i, 2\sqrt{2}),$$

$y_i \in [4/2.51, 2.51]$.

9.6. Dimension Reduction.

Calculation 9.6.1. The polynomial derived for the dimension-reduction argument is positive for $x \in [4, 2.51^2]^6$ and $x \in [4, 2.51^2]^5[4, 8]$.

9.7. Second Partial Bounds. We compute all second partials $\frac{d^2}{dx_i dx_j}$ in terms of x_i , the squares of the edge lengths. We do each computation twice, once for q.r. tets and once for quarters. We compute the second partials of dih, sol, gma volume, and vor volume (the vor analytic volume). Since the scoring functions are linear combinations of sol and the volume terms, we may derive second partial bounds for gma and vor from these.

With the application of additional computer power, these bounds could be improved. These bounds were computed using 16 subdivisions. While using 32 subdivisions would improve the bounds by a factor of 2, perhaps, the time required for the computations increases by a factor of 64.

Calculation 9.7.1. For q.r. tets, the second partials of dih lie in

$$[-0.0926959464, 0.0730008897].$$

Calculation 9.7.2. For quarters, the second partials of dih lie in

$$[-0.2384125007, 0.169150875].$$

Calculation 9.7.3. For q.r. tets, the second partials of sol lie in

$$[-0.0729140255, 0.088401996].$$

Calculation 9.7.4. For quarters, the second partials of sol lie in

$$[-0.1040074557, 0.1384785805].$$

Calculation 9.7.5. For q.r. tets, the second partials of gma volume lie in

$$[-0.0968945273, 0.0512553817].$$

Calculation 9.7.6. For quarters, the second partials of gma volume lie in
 $[-0.1362100221, 0.1016538923]$.

Calculation 9.7.7. For q.r. tets, the second partials of vor volume lie in
 $[-0.1856683356, 0.1350478467]$.

Calculation 9.7.8. For quarters, the second partials of vor volume lie in
 $[-0.2373892383, 0.1994181009]$.

The computed gma second partials then lie in

$$[-0.2119591984, 0.2828323141],$$

for q.r. tets and quarters.

Likewise, the computed vor second partials then lie in

$$[-0.7137209962, 0.8691765157],$$

for q.r. tets and quarters.

APPENDIX A. COMPUTER CODE

I would like to include the C code used in performing the verifications. However, there is simply too much code to include here. I will make the code available electronically [F].

The code is not particularly beautiful. This is due in part to the fact that there is no “natural” representation for interval arithmetic in C. The “operator overloading” available in C++ allows for prettier notation, but extracts a serious performance penalty. For example, there are much more efficient methods for implementing interval arithmetic on polynomials than the binary approach which operator overloading requires. As the speed of execution is very important, I chose more cumbersome notation instead of sleeker, but significantly slower, code. Incidentally, speed was the reason why I chose not to use an external interval arithmetic package.

There is a fair amount of duplication in the code, since it evolved significantly over time, as new methods eclipsed older ones. For example, some of the code is specialized to treat only tetrahedra with acute faces, since this allows for some simplifications which improve the efficiency of the routines. With the development of the Taylor method, these improvements became less significant, but are still part of the code, mostly due to inertia on my part.

Since each verification typically has some unique characteristics, the code for conducting each verification has unique elements. This makes it difficult to represent everything compactly.

The code should be fairly portable. However, rounding control routines vary from platform to platform, as do special commands, like FMADD, the floating-point fused multiply-add command. Therefore, some minor changes will be required to localize the code to a particular platform.

To give the flavor of the essentials of the code, I will include code for computing the solid angle of a tetrahedron, and code for the verification of Calculation 9.4.3.

A.1. Computing the solid angle. By Lemma 8.4.2 of [H3], the formula for the solid angle of a tetrahedron S with edge lengths (y_1, y_2, \dots, y_6) is given by

$$\text{sol}(S) = 2 \arctan\left(\frac{\sqrt{\Delta}}{2a}\right).$$

Here

$$\begin{aligned} a(y_1, y_2, \dots, y_6) = & y_1 y_2 y_3 + \frac{1}{2} y_1 (y_2^2 + y_3^2 - y_4^2) \\ & + \frac{1}{2} y_2 (y_1^2 + y_3^2 - y_5^2) + \frac{1}{2} y_3 (y_1^2 + y_2^2 - y_6^2) \end{aligned}$$

and

$$\begin{aligned} \Delta(x_1, \dots, x_6) = & x_1 x_4 (-x_1 + x_2 + x_3 - x_4 + x_5 + x_6) \\ & + x_2 x_5 (x_1 - x_2 + x_3 + x_4 - x_5 + x_6) \\ & + x_3 x_6 (x_1 + x_2 - x_3 + x_4 + x_5 - x_6) \\ & - x_2 x_3 x_4 - x_1 x_3 x_5 - x_1 x_2 x_6 - x_4 x_5 x_6, \end{aligned}$$

where $x_i = y_i^2$ for $i = 1, \dots, 6$.

Note that the function a is increasing in y_1, y_2 , and y_3 on $[2, 4]$ and is decreasing in the variables y_4, y_5 , and y_6 on the same interval. We use this fact to simplify the interval calculation of a .

We represent an interval t as $[\underline{t}, \bar{t}]$. In C, we represent this interval as a double-precision floating-point array with two elements, `double t[2]`. We define $\underline{t} = \mathbf{t}[0]$ and $\bar{t} = \mathbf{t}[1]$.

If each y_i represents an interval, we denote the cell (y_1, \dots, y_6) in C as a double-precision floating-point array with twelve elements, `double y[12]`. We define $\underline{y}_i = \mathbf{y}[2(i-1)]$, and $\bar{y}_i = \mathbf{y}[2(i-1)+1]$.

We begin with the implementation of Δ . The macros `ROUND_DOWN` and `ROUND_UP` change the rounding direction for floating-point computations. We attempt to take advantage of the polynomial structure, reducing the interval overhead as much as possible.

Essentially, we are taking advantage of the fact that it is much more efficient to compute $a + b + c$ as

$$[\underline{a} + \underline{b} + \underline{c}, \bar{a} + \bar{b} + \bar{c}],$$

since we only need to change the rounding direction once, compared to computing $(a + b) + c$, which would be required by a binary interval arithmetic operator. We therefore avoid much of the function-call overhead, and in addition, we won't cause as many floating-point pipeline stalls, since we don't have to change the rounding direction as often.

```
void i_bigdelta( double x[12], double out[2] )
{
    double pterms[2], nterms[2], p1, p2, p3, p4;

    ROUND_DOWN;
    p1 = x[0]*x[6]*(x[2] + x[4] + x[8] + x[10]);
    p2 = x[2]*x[8]*(x[0] + x[4] + x[6] + x[10]);
    p3 = x[4]*x[10]*(x[0] + x[2] + x[6] + x[8]);
```

```

pterms[0] = p1 + p2 + p3;
p1 = x[0]*x[6]*(x[0] + x[6]);
p2 = x[2]*x[8]*(x[2] + x[8]);
p3 = x[4]*x[10]*(x[4] + x[10]);
p4 = x[4]*(x[2]*x[6] + x[0]*x[8]) + x[10]*(x[0]*x[2] + x[6]*x[8]);
nterms[0] = p1 + p2 + p3 + p4;
ROUND_UP;
p1 = x[1]*x[7]*(x[3] + x[5] + x[9] + x[11]);
p2 = x[3]*x[9]*(x[1] + x[5] + x[7] + x[11]);
p3 = x[5]*x[11]*(x[1] + x[3] + x[7] + x[9]);
pterms[1] = p1 + p2 + p3;
p1 = x[1]*x[7]*(x[1] + x[7]);
p2 = x[3]*x[9]*(x[3] + x[9]);
p3 = x[5]*x[11]*(x[5] + x[11]);
p4 = x[5]*(x[3]*x[7] + x[1]*x[9]) + x[11]*(x[1]*x[3] + x[7]*x[9]);
nterms[1] = p1 + p2 + p3 + p4;
I_SUB( pterms, nterms, out );
/* Only care about simplices for which delta > 0 */
if( out[0] < 0.0 )
    out[0] = 0.0;
if( out[1] < 0.0 )
    out[1] = 0.0;
}

```

By Lemma 8.1.4 of [H3], if Δ is negative, the simplex associated with the squares of the edge lengths (x_1, \dots, x_6) does not exist. We therefore discard simplices with $\Delta < 0$.

We need to compute $\sqrt{\Delta}$. In all of our code, we may assume that the argument of the square root function is non-negative. If part of an interval is negative, we truncate it so `sqrt` won't complain.

```

void i_sqrt( double x[2], double out[2] )
{
    ROUND_DOWN;
    if( x[0] < 0.0 )
        out[0] = 0.0;
    else
        out[0] = sqrt( x[0] );
    ROUND_UP;
    out[1] = sqrt( x[1] );
}

```

We next compute the minimum value of a . We take advantage of the monotonicity relation which we observed previously. In the discussion following Lemma 8.4.2 of [H3], we find that $a > 0$ for any simplex with edges in the interval $[2, 4]$. This fact is obvious for simplices for acute faces. We may therefore adjust the value of `min_a` should it return a negative number.

```

/* min_a( y ) = a( y[0], y[2], y[4], y[7], y[9], y[11] ) */
double min_a( double y[12] )
{
    double y2[12];
    double p1, p2, p3, y123;
    int i;

    ROUND_DOWN;
    for( i=0; i<6; i+=2 )
        y2[i] = y[i]*y[i];
}

```

```

ROUND_UP;
for( i=7; i<12; i+=2 )
    y2[i] = y[i]*y[i];
ROUND_DOWN;
p1 = y2[2] + y2[4] - y2[7];
p2 = y2[0] + y2[4] - y2[9];
p3 = y2[0] + y2[2] - y2[11];
y123 = y[0]*y[2]*y[4];
p1 = y123 + 0.5*(y[0]*p1 + y[2]*p2 + y[4]*p3);
if( p1 < 0.0 )
    p1 = 0.0;
return( p1 );
}

```

Often, we only need one half of the interval bound for a , which is why I separated the routines.

```

/* max_a( y ) = a( y[1], y[3], y[5], y[6], y[8], y[10] ) */

```

```

double max_a( double y[12] )
{
    double y2[12];
    double p1, p2, p3, y123;
    int i;

    ROUND_DOWN;
    for( i=1; i<6; i+=2 )
        y2[i] = y[i]*y[i];
    ROUND_UP;
    for( i=6; i<12; i+=2 )
        y2[i] = y[i]*y[i];
    ROUND_UP;
    p1 = y2[3] + y2[5] - y2[6];
    p2 = y2[1] + y2[5] - y2[8];
    p3 = y2[1] + y2[3] - y2[10];
    y123 = y[1]*y[3]*y[5];
    p1 = y123 + 0.5*(y[1]*p1 + y[3]*p2 + y[5]*p3);
    return( p1 );
}

```

We now compute the solid angle. `ATANERR` is a constant which corrects for the potential error in computing the arctangent.

```

void i_solid( double y[12], double sqrtdelta[2],
             double out[2] )
{
    double max, temp, mina;

    temp = sqrtdelta[0];
    mina = 2.0*max_a( y );
    ROUND_DOWN;
    max = temp/mina;
    out[0] = 2.0*(atan( max ) - ATANERR);

    temp = sqrtdelta[1];
    mina = 2.0*min_a( y );
    ROUND_UP;
    max = temp/mina;
    out[1] = 2.0*(atan( max ) + ATANERR);
}

```

A.2. **A sample verification.** The code for the verification of Calculation 9.4.3 should be representative of how the verifications were conducted.

```

/* octa_gma.c, by Samuel Ferguson, (c) 1997. */

#include "system_headers.h"
#include "sphere.h"
#include "interval.h"
#include "i_sphere.h"
#include "i_bounds.h"
#include "i_taylor.h"
#include "macros.h"

#define MAXDEPTH 32      /* Max recursion depth (was 10) */
#define PARTIALS 1      /* use partials, or not */

#define SUBDIV 2        /* (4) number of subdivisions (1-d) */
#define SUBFRAC 0.5    /* (0.25) 1/SUBDIV (make this exact . . . */

#define MAXLEN 2.51
#define SCORECUT -0.05758859149521 /* -1.04 pt */
#define CUTBD1 2.716
#define CUTBD2 2.81
#define Y4BOUND TW051_HI
#define PEELBD 2.2
#define ALPHA 0.14 /* 0.56/4 */ /* dihedral correction */

/* Even newer bounds:
line1[x_]:= 0.4922197796533495 - 0.3621*x
tetshift[x_]:= 0.253109 - 0.3621*x (eps = 0.07364)
*/

#define INTER1 0.4922197796533495
#define SLOPE1 0.3621

/* External variables */

extern double i_pi_const[2];
extern double i_pi_2_const[2];
extern double i_doct_const[2];
extern double i_two_pi_5_const[2];

/* External prototypes */

void i_init( void );

/* Global variables */

double cellcount;
double verifycount;
double partialcount;
double sccutcount;
double gmacount;
double vorcount;
double dualcount;
double celltotal;
int maxdepth;
int failed;

```

```

double slop;
double twosqrt2;

struct Cell_Info {
    int depth;
    int cell_type;
};

/* Prototypes */

void verifyoctagma( void );
void verify_cell( double tet[12], struct Cell_Info info );

/* Code */

void main( void )
{
    ROUND_NEAR;

    printf("Welcome to sphere packing routines, relation testing division.\n");
    verifyoctagma();
}

void verifyoctagma( void )
{
    int i, n;
    double tet[12];
    double diff, dt;
    time_t tstart, tstop;
    clock_t cstart, cstop;
    char *charptr;
    struct Cell_Info cell_info;

    printf("Welcome to OctaGma. ");
    #if PARTIALS
    printf("Using partials to reduce complexity.\n");
    #else
    printf("Not using partials.\n");
    #endif
    printf("Subdivisions: %d\n\n", SUBDIV);
    printf("Enter slop: ");
    scanf("%lf", &slop);
    printf("\t\tSlop = %g\n", slop );

    i_init(); /* initialize interval constants */

    ROUND_DOWN;
    slop += 0.25*INTER1 + ALPHA*0.5*i_pi_const[0];
    ROUND_NEAR;

    time(&tstart);
    cstart = clock();

    charptr = ctime( &tstart );
    printf("Starting time: \t");
    puts( charptr );
}

```

```

celltotal = 0.0;
for( n=1; n<6; n++ ) {
  printf("Starting case %d:\n", n);
  cellcount = 0.0;
  verifycount = 0.0;
  partialcount = 0.0;
  sccutcount = 0.0;
  vorcount = 0.0;
  gmacount = 0.0;
  dualcount = 0.0;
  maxdepth = 0;
  failed = 0;
  cell_info.depth = 0;
  cell_info.cell_type = -1;

  for( i=0; i<12; i++ )
    tet[i] = 2.0;
  tet[0] = CUTBD1;
  tet[1] = TWOSQRT2_HI;

  switch( n ) {
    case 1:
      tet[1] = CUTBD1; /* tight */
      tet[7] = Y4BOUND;
      tet[9] = PEELBD;
      tet[11] = PEELBD;
      break;
    case 2:
      tet[1] = CUTBD1; /* tight */
      tet[3] = PEELBD;
      tet[5] = PEELBD;
      tet[9] = PEELBD;
      tet[11] = PEELBD;
      break;
    case 3:
      tet[3] = PEELBD;
      tet[7] = Y4BOUND;
      tet[9] = PEELBD;
      break;
    case 4:
      tet[3] = PEELBD;
      tet[5] = PEELBD;
      tet[7] = Y4BOUND;
      break;
    case 5:
      tet[3] = PEELBD;
      tet[5] = PEELBD;
      tet[11] = Y4BOUND;
      break;

    default:
      printf("fell off end: this can't happen\n");
      break;
  }
  verify_cell( tet, cell_info );
  printf("cellcount    = %16.0f\t\t", cellcount);
  printf("maxdepth = %d\n", maxdepth);
  printf("sccutcount  = %16.0f\n", sccutcount);
}

```

```

printf("gmacount      = %16.0f\t\t", gmacount);
printf("vorcount      = %16.0f\n", vorcount);
printf("dualcount      = %16.0f\t\t", dualcount);
printf("verifycount    = %16.0f\n", verifycount);
printf("partialcount    = %16.0f\t\t", partialcount);
diff = cellcount - verifycount - partialcount - sccutcount;
printf("diff          = %16.0f\n", diff);
if( !failed )
    printf("Verification succeeded.\n\n");
else
    printf("MAXDEPTH exceeded.\n\n");
celltotal += cellcount;
} /* end case loop */

ROUND_NEAR;
time(&tstop);
cstop = clock();
printf("Done.\n");
diff = ( (double) (cstop - cstart) )/CLOCKS_PER_SEC;
charptr = ctime( &tstop );
printf("Ending time:   \t");
puts( charptr );
#if DA_SYSTEM == 2
    dt = ( double ) tstop - tstart;
#else
    dt = difftime( tstop, tstart );
#endif
printf("Elapsed time: %g seconds\n", dt);
printf("diff = %g\t\t", diff);
printf("%g cells per second\n\n", celltotal/dt);
}

void verify_cell( double y[12], struct Cell_Info info )
{
    int i, j, bounds[6], n0, n1, n2, n3, n4, n5;
    int check, rel[5];
    double diff[6], t[12], val;
    double sc;
    double x[12], yp[12];
    double relconst[5], rel_val[2];
    double outvals[10];

    /* If part of the verification has already failed, bail. */
    if( failed )
        return;

    cellcount += 1.0;

    /* Compute square of edge lengths */

    ROUND_UP;
    for( i=1; i<12; i+=2 )
        x[i] = y[i]*y[i];
    ROUND_DOWN;
    for( i=0; i<12; i+=2 )
        x[i] = y[i]*y[i];

```

```

if( x[1] > 8.0 )
    x[1] = 8.0;

/* First try to verify over the current cell. */

/* Determine cell type */
check = info.cell_type;
if( check == -1 ) { /* indeterminate */
    check = octa_scoring( x );
    info.cell_type = check;
}

if( check == 1 ) {
    gmacount +=1.0;
}
else if( check == 0 ) {
    vorcount += 1.0;
    return;
}
else
    dualcount += 1.0;

/* Score cell properly */
/* Order:  sol,  gma,  vor,  octavor,  dih */
/*          0    1  2          3    4 */
for( i=0; i<5; i++ ) {
    rel[i] = 0;
    relconst[i] = 0.0;
}
rel[1] = 1;
relconst[0] = SLOPE1;
relconst[1] = 1.0;
relconst[4] = ALPHA;

/* val = sc + SLOPE1*sph + ALPHA*dih */
t_composite( rel, relconst, y, x, rel_val, t,
    outvals );

val = rel_val[1];
sc = outvals[3];

/* Discard cells with low score */
if( sc < SCORECUT ) {
    sccutcount++;
    return;
}

/* Attempt verification */
if( val < slop ) {
    verifycount += 1.0;
    return;
}

/* if verification fails, try to bump off, or at least
   reduce dimension */

for( i=0; i<12; i++ )

```

```

yp[i] = y[i]; /* copy y */

#if PARTIALS

/* Score cell properly (find min score) */
if( check == 1 && outvals[2] > SCORECUT ) {
    /* t contains the relation partials */
    ROUND_NEAR;
    j = 0;
    for( i=0; i<6; i++ ) {
        diff[i] = yp[j+1] - yp[j]; /* compute differentials */
        j += 2;
    }
    /* Long edge is the first one, don't do that here. */
    /* Do edges 2 and 3 */
    j = 1;
    for( i=2; i<6; i+=2 ) {
        n0 = i + 1;
        if( diff[j] > 0.0 ) { /* ignore tight spots */
            if( t[n0] < 0.0 ) {
                if( yp[i] != 2.0 ) {
                    partialcount += 1.0;
                    return; /* bumped off */
                }
            }
            else
                yp[n0] = 2.0; /* reduced dimension */
        }
        else {
            if( t[i] > 0.0 ) {
                if( yp[n0] != PEELBD ) {
                    partialcount += 1.0;
                    return; /* bumped off */
                }
            }
            else
                yp[i] = PEELBD; /* reduced dimension */
        }
    }
}
j++;
}

/* Do edges 5 and 6 */
j = 4;
for( i=8; i<12; i+=2 ) {
    n0 = i + 1;
    if( diff[j] > 0.0 ) { /* ignore tight spots */
        if( t[n0] < 0.0 ) {
            if( yp[i] != 2.0 ) {
                partialcount += 1.0;
                return; /* bumped off */
            }
        }
        else
            yp[n0] = 2.0; /* reduced dimension */
    }
    else {
        if( t[i] > 0.0 ) {
            if( yp[n0] != PEELBD ) {
                partialcount += 1.0;
                return; /* bumped off */
            }
        }
    }
}

```

```

    }
    else
        yp[i] = PEELBD; /* reduced dimension */
    }
}
j++;
}
/* Do edge 4 */
j = 3;
i = 6;
n0 = 7;
if( diff[j] > 0.0 ) { /* ignore tight spots */
    if( t[n0] < 0.0 ) {
        if( yp[i] != 2.0 ) {
            partialcount += 1.0;
            return; /* bumped off */
        }
        else
            yp[n0] = 2.0; /* reduced dimension */
    }
    else {
        if( t[i] > 0.0 ) {
            if( yp[n0] != Y4BOUND ) {
                partialcount += 1.0;
                return; /* bumped off */
            }
            else
                yp[i] = Y4BOUND; /* reduced dimension */
        }
    }
}
/* Now consider the long edge. */
/*
j = 0;
i = 0;
n0 = 1;
*/
if( diff[0] > 0.0 ) { /* ignore tight spots */
    if( t[1] < 0.0 ) {
        if( yp[0] != CUTBD1 ) {
            partialcount += 1.0;
            return; /* bumped off */
        }
        else
            yp[1] = CUTBD1; /* reduced dimension */
    }
    else {
        if( t[0] > 0.0 ) {
            if( yp[1] != TWOSQRT2_HI ) {
                partialcount += 1.0;
                return; /* bumped off */
            }
            else
                yp[0] = TWOSQRT2_HI; /* reduced dimension */
        }
    }
}
}
}

```

```

    }
#endif
if( info.depth < MAXDEPTH ) {
    /* If all else fails, subdivide. */
    info.depth++;
    if( info.depth > maxdepth )
        maxdepth = info.depth;
    ROUND_NEAR;
    j = 0;
    for( i=0; i<6; i++ ) { /* scaled differentials */
        diff[i] = SUBFRAC*(yp[j+1] - yp[j]);
        j += 2;
        if( diff[i] > 0.0 )
            bounds[i] = SUBDIV;
        else
            bounds[i] = 1;
    }
    for( n0=0; n0<bounds[0]; n0++ ) {
        val = yp[0];
        t[0] = val + n0*diff[0];
        t[1] = val + (n0+1)*diff[0];
        for( n1=0; n1<bounds[1]; n1++ ) {
            val = yp[2];
            t[2] = val + n1*diff[1];
            t[3] = val + (n1+1)*diff[1];
            for( n2=0; n2<bounds[2]; n2++ ) {
                val = yp[4];
                t[4] = val + n2*diff[2];
                t[5] = val + (n2+1)*diff[2];
                for( n3=0; n3<bounds[3]; n3++ ) {
                    val = yp[6];
                    t[6] = val + n3*diff[3];
                    t[7] = val + (n3+1)*diff[3];
                    for( n4=0; n4<bounds[4]; n4++ ) {
                        val = yp[8];
                        t[8] = val + n4*diff[4];
                        t[9] = val + (n4+1)*diff[4];
                        for( n5=0; n5<bounds[5]; n5++ ) {
                            val = yp[10];
                            t[10] = val + n5*diff[5];
                            t[11] = val + (n5+1)*diff[5];
                            verify_cell( t, info );
                            ROUND_NEAR;
                        }
                    }
                }
            }
        }
    }
} else { /* exceeded MAXDEPTH */
    failed = 1;
    ROUND_NEAR;
    printf("Cell failed:\n");
    printf("val = %g\n", val - slop);
    printf("sc = [%g, %g]\n",
        outvals[2], outvals[3]);
    for( i=0; i<12; i+=2 )
        printf("%0.18f\t%0.18f\n", y[i], y[i+1]);
}

```

```

}
}

```

APPENDIX B. RESULTS

The output of each verification contains information about the number of cells considered, how the cells were scored, how many cells were discarded and why, and the number of recursive subdivisions. I will make the results of each computation available electronically [F]. As a representative sample, I include the output from Calculation 9.4.3.

This calculation has several cases, which arise from the dimension-reduction argument. It is a relatively simple calculation, since only several thousand cells had to be considered. The inequality which we prove is tighter than that exhibited (and required) earlier in the paper. The “slop” value refers to the amount of relaxation from the ideal bound.

```

Welcome to sphere packing routines, relation testing division.
Welcome to OctaGma. Using partials to reduce complexity.
Subdivisions: 2

```

```

Enter slop: 1.0e-5
      Slop = 1e-05
Starting time: Sun Jun 29 11:03:12 1997

```

```

Starting case 1:

```

```

cellcount   =      363   maxdepth = 5
sccutcount  =      137
gmacount    =      363   vorcount   =           0
dualcount   =           0   verifycount =          180
partialcount =           0   diff      =           46

```

```

Verification succeeded.

```

```

Starting case 2:

```

```

cellcount   =      609   maxdepth = 4
sccutcount  =         66
gmacount    =      609   vorcount   =           0
dualcount   =           0   verifycount =          504
partialcount =           0   diff      =           39

```

```

Verification succeeded.

```

```

Starting case 3:

```

```

cellcount   =     3959   maxdepth = 9
sccutcount  =     1398
gmacount    =     3406   vorcount   =           0
dualcount   =         553   verifycount =         2297
partialcount =           4   diff      =          260

```

```

Verification succeeded.

```

```

Starting case 4:

```

```

cellcount   =     3203   maxdepth = 9
sccutcount  =     1150
gmacount    =     2738   vorcount   =           0
dualcount   =         465   verifycount =         1838
partialcount =           1   diff      =          214

```

```

Verification succeeded.

```

Starting case 5:

cellcount	=	2025	maxdepth =	9	
sccutcount	=	39			
gmacount	=	1366	vorcount	=	144
dualcount	=	515	verifycount	=	1701
partialcount	=	1	diff	=	284

Verification succeeded.

Done.

Ending time: Sun Jun 29 11:03:20 1997

Elapsed time: 8 seconds

diff = 7.83333 1269.88 cells per second

Some verifications require the consideration of millions of cells. Without the use of dimension-reduction and Taylor methods, they could require billions of cells, or could even lie beyond our current computer resources.

REFERENCES

- [F] S. P. Ferguson, <http://www.math.lsa.umich.edu/~samf> .
- [F&H] S. P. Ferguson, T. C. Hales, A formulation of the Kepler conjecture, math.MG/9811072
- [H1] T. C. Hales, Remarks on the density of sphere packings in three dimensions, *Combinatorica*, 1993, 13:181-197
- [H2] T. C. Hales, The sphere packing problem, *J. Comput. Appl. Math.*, 1992, 44:41-76
- [H3] T. C. Hales, Sphere packings, I, *Discrete Comput. Geom.*, 1997, 17:1-51, math.MG/9811073
- [H4] T. C. Hales, Sphere packings, II, *Discrete Comput. Geom.*, 1997, 18:135-149, math.MG/9811074
- [IEEE] IEEE Standard for Binary Floating-Point Arithmetic, ANSI/IEEE Std. 754-1985, IEEE, New York.

DEPARTMENT OF MATHEMATICS, UNIVERSITY OF MICHIGAN, ANN ARBOR, MI 48109

E-mail address: samf@math.lsa.umich.edu

URL: <http://www.math.lsa.umich.edu/~samf>